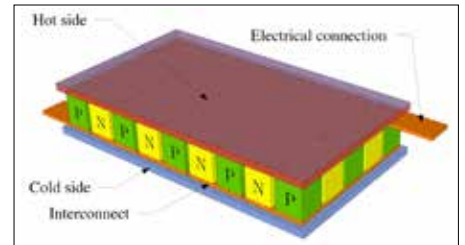
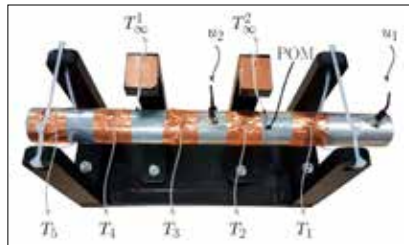
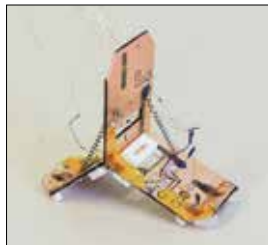
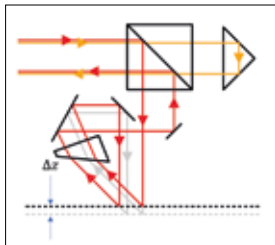
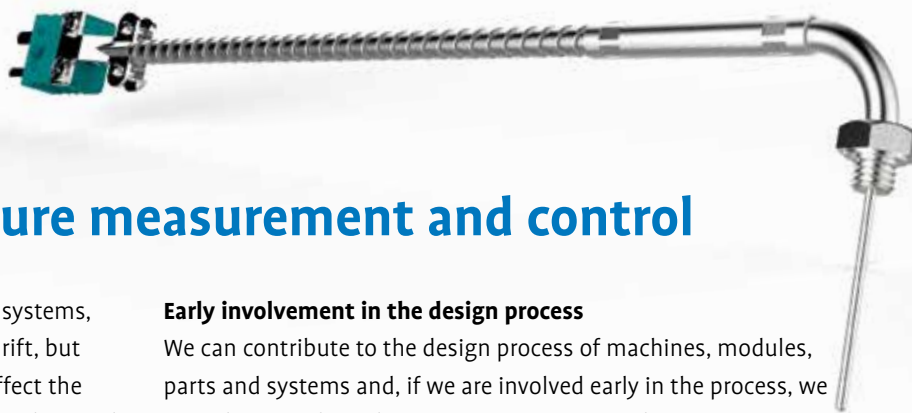


PROFESSIONAL JOURNAL ON PRECISION ENGINEERING

A large, modern laboratory facility, likely a synchrotron or X-ray free-electron laser (XFEL) beamline. The foreground features a complex assembly of white and black modular equipment, heavily cabled with numerous green, blue, and white wires. The equipment is mounted on a black metal frame with red safety components. In the background, a person is seated at a workstation with multiple computer monitors, operating the facility. The room has a high ceiling with recessed lighting and a clean, industrial aesthetic.



- # DSPE



The specialist in temperature measurement and control

Temperature is an important parameter in many processes, systems, machines or parts of machines. Temperature variations or drift, but also unwanted temperature differences, can considerably affect the performance of a machine or system. Proper measurement and control of temperature in a process has a positive effect on the lifespan of machines, ensures fewer downtime and improves performance.

Customized temperature sensors

Tempcontrol develops and manufactures customized and standard temperature sensors, specializing in tailor made solutions. With over 40 years of experience, we are always able to find the right solution for each specific application. A quick response time, high accuracy, long-term stability, resistance to high or low temperatures, nearly anything is possible.

Early involvement in the design process

We can contribute to the design process of machines, modules, parts and systems and, if we are involved early in the process, we can advise on the right temperature sensor and instrumentation.

At our location we have a production department, a warehouse, a cleanroom and a calibration and research lab. Here we develop, produce, measure, optimize, calibrate and stabilize temperature sensors and instrumentation. Testing (long-term) and investigation of temperature sensors is also possible.

In addition, we can provide high-quality instrumentation and precision measuring equipment from quality brands such as AsconTecnologic, ASL/Wika, Dostmann, Inor, MBW, Giussani, Kambic and Optocon.

Temperature sensors in many designs



Handheld instruments



Transmitters, isolators, controllers



Climatic chambers, calibration baths



Precision measuring equipment



Accessories



PUBLICATION INFORMATION

Objective

Professional journal on precision engineering and the official organ of DSPE, the Dutch Society for Precision Engineering. Mikroniek provides current information about scientific, technical and business developments in the fields of precision engineering, mechatronics and optics. The journal is read by researchers and professionals in charge of the development and realisation of advanced precision machinery.



Publisher

DSPE
Annemarie Schrauwen
High Tech Campus 1, 5656 AE Eindhoven
PO Box 80036, 5600 JW Eindhoven
info@dspe.nl, www.dspe.nl

Editorial board

Prof.dr.ir. Just Herder (chairman, Delft University of Technology, University of Twente),
Servaas Bank (VDL ETG), B.Sc.,
ir.ing. Bert Brals (Sioux Mechatronics),
dr.ir. Dannis Brouwer (University of Twente),
Maarten Dekker, M.Sc. (Philips),
Otte Haitisma, M.Sc. (Demcon),
ing. Ronald Lamers, M.Sc. (Thermo Fisher Scientific),
Erik Manders, M.Sc. (Philips Innovation Services),
dr.ir. Pieter Nuij (NTS-Group),
dr.ir. Gerrit Oosterhuis (VDL ETG),
Maurice Teuwen, M.Sc. (Janssen Precision Engineering)

Editor

Hans van Eerden, hans.vaneerden@dspe.nl

Advertising canvasser

Gerrit Kulsdom, Sales & Services
+31 (0)229 – 211 211, gerrit@salesandservices.nl

Design and realisation

Drukkerij Snep, Eindhoven
+31 (0)40 – 251 99 29, info@snep.nl

Subscription

Mikroniek is for DSPE members only.
DSPE membership is open to institutes, companies, self-employed professionals and private persons, and starts at € 80.00 (excl. VAT) per year.

Mikroniek appears six times a year.

© Nothing from this publication may be reproduced or copied without the express permission of the publisher.

ISSN 0026-3699



The main cover photo (featuring a Thermo Fisher Titan electron microscope outside an opened acoustic enclosure) is courtesy of Thermo Fisher (photo: Leo Koomen). Read the article on page 12 ff.

IN THIS ISSUE

THEME: THERMAL CONTROL

05

Peltiers for precision actuation

A generic input-output linearising feedback law for thermo-electric coolers has been investigated, while explicitly modelling the effects that degrade the control performance in a practical set-up.

12

Thermally induced deformations in electron microscopy

Modelling thermal systems from experimental data, i.e. system identification, is challenging due to large transients, large time scales, excitation signal limitations, large environmental disturbances, and nonlinear behaviour. An identification framework has been developed to address these issues.

20

Thermal qualification of precision systems

Thermal qualification of a temperature-conditioned heat shield for a precision motion system has been performed using modelling and measurement tools.

26

Innovation – Encoders graduating to extreme precision

Design, implementation and performance of new optical heterodyne encoder systems, which achieve sub-nm displacement measurements for stages moving at over 8 m/s.

32

Event report – 11th Expert Days on Service Robotics

Topics include healthcare robot applications, learning, reconfigurable robots, safety, and cobots, i.e. collaborative robots.

37

Manufacturing – Multitasking machines

Both additive and subtractive shaping without reclamping.



37



41

FEATURES

04 EDITORIAL

Pieter Kappelhof (technology manager Hittech Group, vice president DSPE) on the DSPE Thermomechanics website and the engineer's search for knowledge and community.

19 UPCOMING EVENTS

Including: Dutch System Architecting Conference.

40 ECP2 COURSE CALENDAR

Overview of European Certified Precision Engineering courses.

41 NEWS

Including: An AM platform for micro-/nanomanufacturing.

46 DSPE

Including: Preview of Precision-in-Business Day at NTS.

IN CONTROL OF THERMOMECHANICS, IN SEARCH OF KNOWLEDGE AND COMMUNITY

Thermomechanics is one of the disciplines that is crucial for successfully designing precision systems, especially optical systems. Thermal loads always lead to drift, which can 'ruin' precision. Hence, thermal control is needed to safeguard these systems' precision performance.

Several industry trends are increasing the relevance of thermomechanics: the demand for higher throughputs in production processes is fuelling an ongoing quest for sources, like lasers or the EUV source, with higher power, while alternatively, the demand for higher accuracies requires more stable systems exhibiting less drift – or at least drift behaviour that is more predictable, for incorporation into thermal control. A third trend for which thermomechanics is highly relevant is the increasing demand for extreme environments, like vacuum or cryogenics, which are often required for taking the next step in research or making new industrial applications possible.

In response to these considerations, eight years ago DSPE initiated a Special Interest Group (SIG) on thermomechanics. One of the things we found was that what information there was on the internet concerning thermomechanics was limited. With DSPE being what it is, an organisation by engineers for engineers, the SIG set out to gather and present information on thermomechanics in a structured way on the DSPE website.

Over a two-year period we created a website with 60 pages of content on modelling, analysis and measurement. We focused on practical usability, so the website offers calculators, rules of thumb, relevant material data, links and articles. Since the release of this 'thermomechanics website', half of the visitors to the DSPE website (47,000 annually) specifically target the thermomechanics pages. Currently, we are working on an update of this substantial knowledge base.

The success of this thermomechanics corner resulted in DSPE deciding to extend its website with additional relevant and unique knowledge for precision engineers, on subjects like 'dynamics for precision' and vacuum technology. In general, we all recognise the fact that engineers searching on the internet for specialist items only find limited knowledge. Google or any regular search engine will give an answer, when it concerns standard knowledge, in just a split second; however, when looking for specialist knowledge, one can be lost for hours on the internet without finding the right information.

Therefore, we are going to work on a better search facility for precision engineers, using expertise including artificial intelligence and data mining. This will help engineers to improve their research or product development process, while also lead to strengthening the virtual community of precision engineers.

We invite all our readers to help generate the content we all need, as well as to assist in working on the DSPE website and to come up with ideas for building a virtual community of precision engineers. Sharing and collaborating are among the strengths of our industry – and most certainly of DSPE.

Pieter Kappelhof

Technology manager Hittech Group, vice president DSPE
pkappelhof@hittech.com



PELTIER FOR PRECISION ACTUATION

Peltier elements, i.e. thermo-electric coolers, are attracting more and more attention for application in high-precision systems where they enable active heat exchange and sub-zero [°C] thermal conditioning. Linear or switching PID controllers are commonly used for their control because of their simplicity in both design and implementation. However, due to their nonlinear behaviour, controlling the cold-side temperature of peltiers isn't simple. As such, Philips Innovation Services investigated a generic input-output linearising feedback law for Peltier devices, while explicitly modelling the effects that degrade the control performance in a practical set-up.

ROB VAN GILS

Introduction

Both consumer electronics and professional equipment alike are becoming increasingly reliant on precise thermal management. Challenges range from (air-only) high-heat-flux cooling, e.g. for increased efficiencies in high-power LED devices [1], to precise thermal conditioning of high-performance components, e.g. in handheld diagnostics platforms for the world's common diseases [2, 3]. As such, thermal control is gaining more attention in the design of these devices.

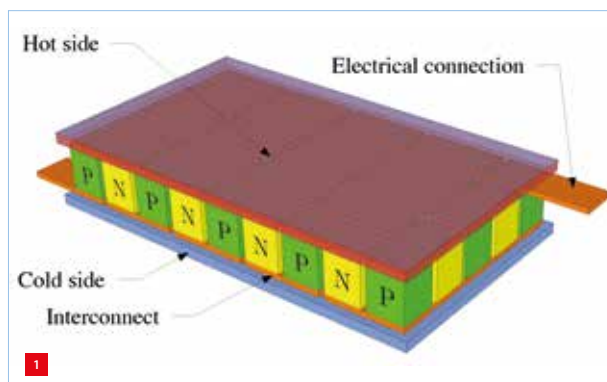
Peltier elements – or 'peltiers' – are thermoelectric coolers (TECs) that can be used either for heating or for cooling. Their main advantages compared to, e.g., a vapour-compression system are their lack of moving parts or circulating liquid, invulnerability to potential leaks, and their small size and flexible shape. This makes them ideal as thermal actuators. As a result, the devices are also gaining more attention for application in high-precision systems, where they enable active heat exchange and sub-zero [°C] thermal conditioning. The disadvantages of peltiers are their high cost, poor power efficiency, sensitivity to mechanical stresses and high currents.

TECs operate based on the Peltier effect, more commonly referred to as the thermoelectric effect. A Peltier device has two sides, connected by thermoelectric legs or pellets, i.e. pairs of N- and P-type semiconductors, which are placed thermally in parallel and electrically in series (see Figure 1). When a DC current flows through the device, it brings heat from one side to the other, so that one side gets cooler while the other gets hotter, generating a 'hot' and a 'cold' side. The hot side is attached to a heat sink so that it remains close to ambient temperature, while the cold side falls below room temperature, see for example [4].

Thermal control/actuation by Peltier devices has been investigated in a wide variety of studies [5]. Most of them focus on effective control of the Peltier cold side (see for example [6-8]). Mathematical models describing the thermal behaviour of Peltier elements can be found in among others [4, 5, 7].

Although various control strategies have been studied, the linear proportional-integral-differential (PID) controllers or switching PID controllers (i.e., where varying parameters are used, e.g. gain scheduling) are commonly used for their simplicity in both design and implementation [8]. However, due to their nonlinear behaviour, controlling the cold-side temperature of peltiers isn't simple. Linear PID control might work in some cases, but isn't robust (see [7]). On the other hand, other studies that consider nonlinear controller techniques don't take into account practical limitations in their controller design.

Therefore, this study investigates a generic input-output (IO) linearising feedback law for Peltier devices, while explicitly modelling the effects that degrade the control



Peltier (or thermoelectric cooler) schematic. (Source: michbich, Wikipedia, commons.wikimedia.org/w/index.php?curid=9076557)

AUTHOR'S NOTE

Rob van Gils is senior technologist Thermal & Flow at Philips Innovation Services in Eindhoven (NL).

rob.van.gils@philips.com
www.innovationservices.philips.com

performance in a practical set-up. An IO linearisation scheme is a feedback law that introduces a new virtual input which relates linearly to the output, in this case the bottom plate temperature. This results in increased performance and larger robustness regimes (see also [9]).

Methodology

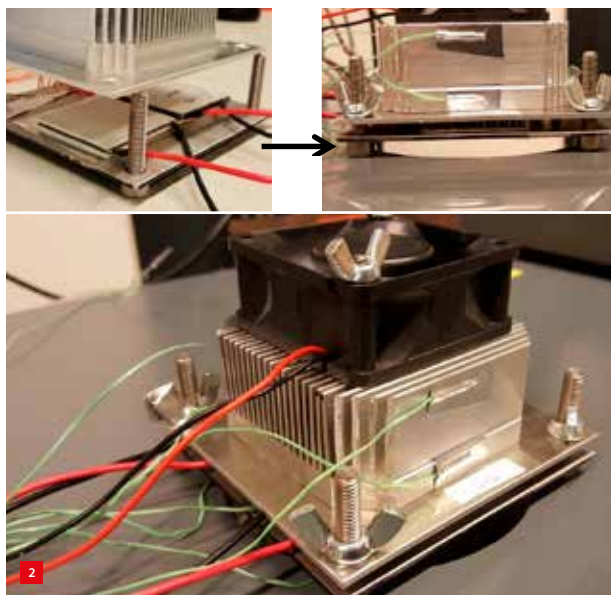
Experimental set-up

This study investigates the practical effectiveness of the IO linearising feedback law by means of a simple test set-up representative of part of a handheld diagnostic device. The set-up is shown in Figure 2. It consists of a stainless steel bottom plate that is divided into two sections that must be thermally controlled individually. To this end, two peltiers are placed between the bottom plate and the aluminium top plate. The latter is connected to a fanned heat sink (HS).

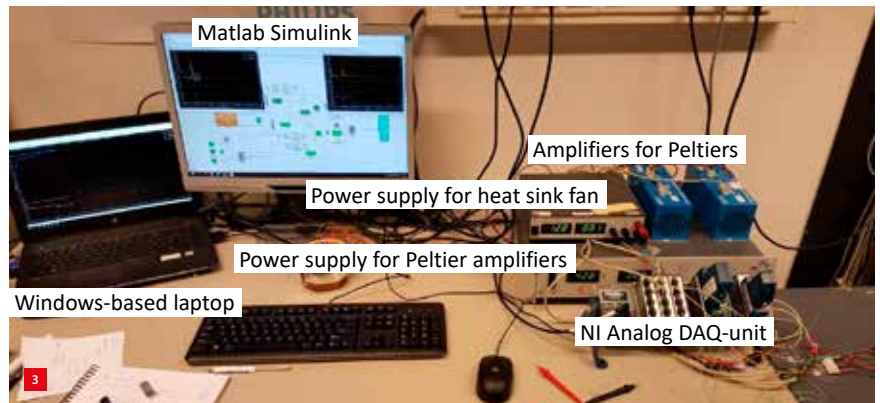
The set-up is controlled using a thermal control platform: a Windows-based computer running Matlab Simulink with software developed in-house to communicate with a USB-based National Instruments DAQ unit for importing and exporting signals (see Figure 3). The Matlab Simulink environment allows for quick and flexible controller design for every set-up. Moreover, it allows for the use of standard control theory due to the extensive systems control toolbox available in Matlab.

Thermo-dynamical model

In order to calculate appropriate controller settings, the experimental set-up is modelled using the Philips Advanced Lumped Mass (PALM) tool, i.e. a set of Matlab macros developed in-house to facilitate efficient lumped-mass modelling. Figure 4 presents a schematic overview of the model of the set-up. The top and bottom plate are divided



Experimental set-up.

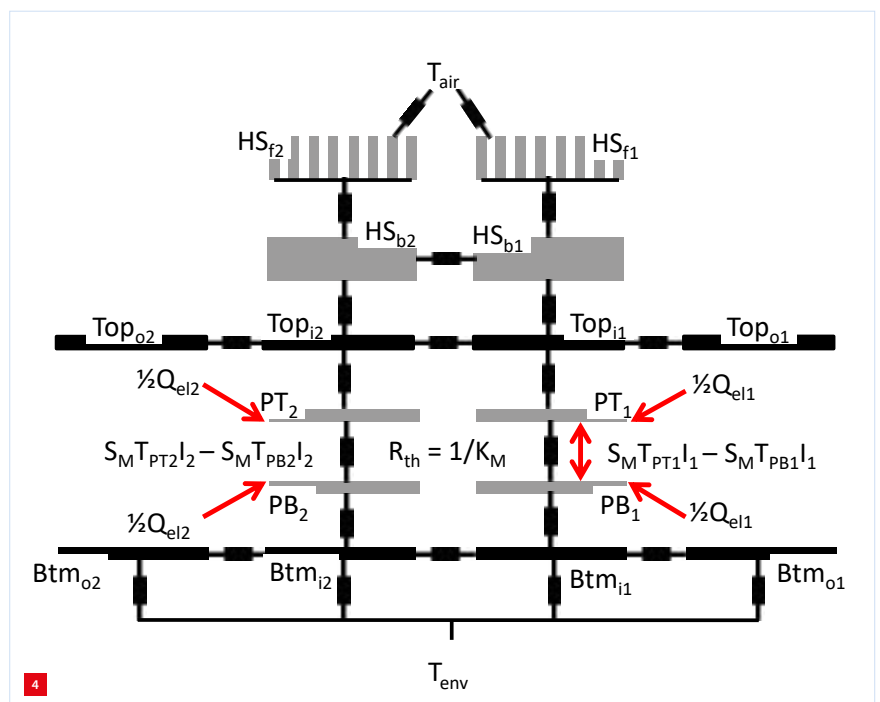


Data acquisition set-up.

into four masses each: two directly adjacent to the peltiers and one mass to represent the plate around each TEC. The HS is divided into a left and right side, and base and fins. The modelling details in connecting the lumped masses are omitted here since these masses can be simply connected via linear thermal resistances. Instead, only the mathematical relations describing the peltier thermal behaviour are discussed (see the box).

Set-up identification and model validation

The temperature-averaged parameters for the peltiers considered are determined using the thermal control platform: $S_M = 0.0509 \text{ V/K}$, $R_M = 3.34 \text{ } \Omega$, $K_M = 0.394 \text{ W/K}$. The set-up contains two peltiers that can be actuated individually. To validate the model, both peltiers are subjected to different input currents and both the resulting peltier voltages as well as the cold-side temperatures are logged and compared to simulations.



Schematic of the lumped-mass model.

Peltier thermal behaviour

If a DC current runs through the Peltier device, heat is extracted from/dumped on the cold/hot side by the Peltier effect and the Seebeck effect. The amount of heat is quantified by the device's Seebeck coefficient, S_M , the DC current, I , and the temperature of the cold/hot side, T_c/T_h , via:

$$\begin{aligned} Q_{peltier,c} &= S_M T_c I \\ Q_{peltier,h} &= S_M T_h I \end{aligned} \quad (1)$$

Besides the heat pumped from the cold to the hot side, heat is also generated in the thermoelectric pairs due to electrical losses, of which half will flow to the hot side and half to the cold side. The heat generated, Q_{el} , is quantified by the DC current and the device resistivity R_M via $Q_{el} = R_M I^2$. Finally, heat is transported from the hot to the cold side due to thermal conduction caused by the temperature gradient over the legs. This leakage is quantified by the device thermal conductivity K_M and equals $Q_{leak} = K_M(T_h - T_c)$.

The differential equations governing the hot- and cold-side temperature then readily follow from these heat flows, yielding a nonlinear and non-affine Peltier model:

$$m_h c_{p,h} \dot{T}_h = S_M T_h I + \frac{1}{2} R_M I^2 - K_M(T_h - T_c) \quad (2)$$

$$m_c c_{p,c} \dot{T}_c = -S_M T_c I + \frac{1}{2} R_M I^2 + K_M(T_h - T_c) \quad (3)$$

Here, T_h and T_c are the hot- and cold-plate temperature, respectively. Biot and Fourier number analyses show that this approach is valid in the parameter space of interest. Moreover, numerical analyses indicate that not modelling the thermoelectric legs introduces only a small error. The total model of the set-up yields:

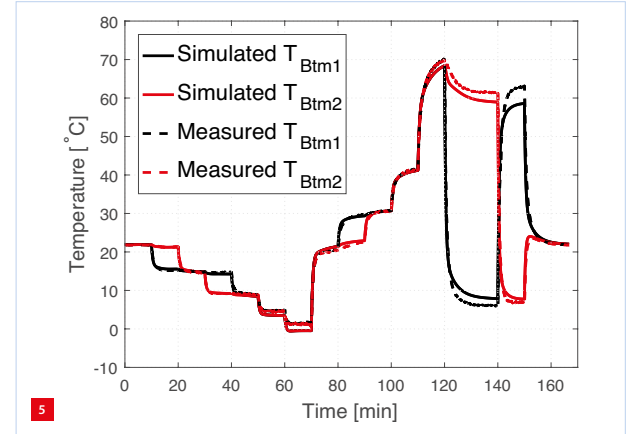
$$E \dot{x} = Ax + Bu + F_{nl} \quad (4)$$

Here, the state vector x (size 16x1) contains the temperatures of the 16 lumped masses, and the input vector u (2x1) contains the external temperatures T_{env} and T_{air} . Furthermore, the matrix E contains the thermal capacities of the masses: A is the system matrix and B the input matrix. Finally, F_{nl} equals:

$$F_{nl} = \begin{bmatrix} S_M x_1 I_1 + \frac{1}{2} R_M I_1^2 - K_M(x_1 - x_2) \\ -S_M x_2 I_1 + \frac{1}{2} R_M I_1^2 + K_M(x_1 - x_2) \\ S_M x_3 I_2 + \frac{1}{2} R_M I_2^2 - K_M(x_3 - x_4) \\ -S_M x_4 I_2 + \frac{1}{2} R_M I_2^2 + K_M(x_3 - x_4) \\ 0 \end{bmatrix} \quad (5)$$

Here:

- x_1 = top plate peltier 1
- x_2 = bottom plate peltier 1
- x_3 = top plate peltier 2
- x_4 = bottom plate peltier 2



Temperatures: measurement vs. simulation.

The results are shown in Figure 5. The simulated values clearly correspond very well with the measured values. Moreover, the simulated and measured resulting peltier voltages also overlap (not shown in the figure), establishing the validity of the model. Hence, the model can be used to investigate different controller techniques and synthesise controller parameters.

Input-output linearisation

Due to the nonlinear nature of the peltier dynamics, the linear control theory is valid only in a very narrow operating range. Unstable behaviour of a previously stable plant can occur rapidly if the heat load at the peltier bottom is shortly increased or if a different temperature setpoint is required.

Theory

An IO linearising feedback is a control strategy in which the input current is chosen such that the relation between a new input u and the output (in this case T_{PB1} : the bottom of peltier 1) is linear. The main advantage of this strategy is that a linear controller can be designed that is stable in the entire operating range and has the same behaviour (i.e. with respect to settling time, overshoot, etc.) for different setpoints.

The input current to the i -th peltier can be described as:

$$I_i = \frac{S_M T_{PB1}}{R_M} - \sqrt{\frac{S_M^2 T_{PB1}^2}{R_M^2} + \frac{u_i}{1/2 R_M}} \quad (6)$$

Substituting this in Equation 5 yields for the second element of the vector F_{nl} :

$$F_{nl,2} = u_1 + K_M(x_1 - x_2) \quad (7)$$

Note that this linearises the entire differential equation (DE) that governs the peltier bottom temperature. Now u_1 is taken as:

$$u_1 = -\frac{1}{\tau_{c1}}(T_{PB1} - T_{set1}) - K_M(x_1 - x_2) - A_{2,:} x \quad (8)$$

Then the DE for the peltier bottom temperature reduces to a first-order linear response with time constant τ_{ci} . Here $A_{2,:}$ means only the second row of the matrix A is considered. The same approach can be followed to linearise the input-output behaviour for the second peltier.

Practice

As discussed above, ideally the peltier bottom temperatures can be set to follow a reference with a given time constant. However, there are a few limitations in practice.

Firstly, the input u_i in Equation 6 must satisfy:

$$u_i \geq -\frac{S_M^2 T_{PBi}^2}{2R_M} \quad (9)$$

This is in order for the square root term in Equation 6 to be ≥ 0 . With this square root term equal to 0, the input current reduces to $I = S_M T_{PBi} / R_M$, which equals the optimal current for which the net heat extraction from the cold side is maximal. Higher currents would lead to more heat dissipation and thus a smaller net heat extraction. This effect is known to cause thermal runaway in PID-controlled peltier set-ups.

Secondly, in practice not all lumped-mass temperatures can be measured, while they are required in Equation 8 to reduce the DE to a first-order linear system. Moreover, the controlled temperature, T_{PBi} , is often not accessible. In our case, it must be replaced with the bottom plate temperature, T_{Btmi} , instead.

Thirdly, the modelling might not be ideal and any effort to reduce the DEs for the peltier bottoms to a first-order linear system is in vain. Therefore, it is better to extend the input u_i with a PI-control scheme, which eliminates any steady-state errors in the closed-loop behaviour that result from these model uncertainties:

$$u_i = -\frac{1}{\tau_{ci}}(T_{Btmi} - T_{set,i}) - K_I e_I - K_M(T_{HSbi} - T_{Btmi}) \quad (10)$$

Here, $e_I = T_{Btmi} - T_{set,i}$. Note that here T_{Btmi} equals the temperature of the bottom plate (of the set-up) directly under the peltier, rather than the peltier bottom temperature, which is given by T_{PBi} .

Note that the limitation on the input u_i remains (see Equation 9). In Equation 10, e_I (subscript I for Integral action) is the integral of the tracking error, thus generating an I-action in the control law u_i , with K_I the I-action controller gain (see e.g. [10]). The implemented I-action in particular introduces standard linear control issues like finding a compromise between settling time and overshoot.

Experimental results

The practically feasible control law, Equation 10, is implemented in the Simulink scheme that drives the Peltier devices. To show its effectiveness, the peltiers are set to follow three reference signal combinations.

Sinusoidal reference tracking

In the first combination, the cold side of the first peltier is to follow a sinusoid with an amplitude of 4 K, a mean at 18 °C and a period time of 300 s, while the second TEC must follow a sinusoid with an amplitude of 10 K, a mean at 22 °C and a period time of 400 s. The reference signals are given by:

$$\begin{aligned} R_1(t) &= 18 + 4 \cdot \sin(2\pi/300 \cdot t) \\ R_2(t) &= 22 + 10 \cdot \sin(2\pi/400 \cdot t) \end{aligned} \quad (11)$$

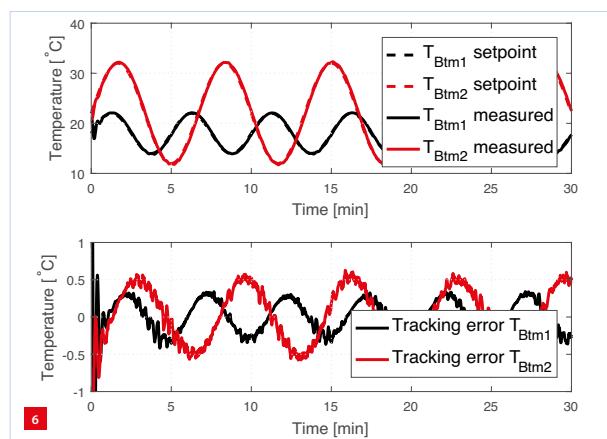
Figure 6 presents the results of the experiment. As can be seen, both peltiers follow their reference without being influenced by the setpoint of the other peltier. The tracking error is in the order of 5%. Note that the absolute tracking error is highly variable under the amplitude and frequency of the reference and that relatively a lot of mass must be thermally cycled in this set-up due to the stainless steel bottom plate under the peltiers.

Pulsed reference tracking

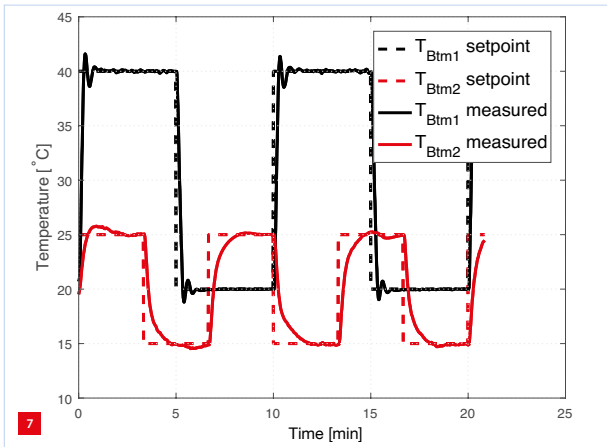
In the second setpoint combination, the peltiers are set to follow pulses. The reference signals are defined by:

$$\begin{aligned} R_1(t) &= 30 + 10 \cdot \text{sign}(\sin(2\pi/600 \cdot t)) \\ R_2(t) &= 20 + 5 \cdot \text{sign}(\sin(2\pi/400 \cdot t)) \end{aligned} \quad (12)$$

It is commonly known in linear control that a compromise between settling time and overshoot must always be made with PI control. Therefore, in this experiment the first



Responses of the set-up's bottom plate temperature directly under the peltiers, for temperature setpoints following Equation 11. Top: bottom plate temperatures. Bottom: tracking errors.



Responses of the set-up's bottom plate temperature directly under the peltiers, for temperature setpoints following Equation 12.

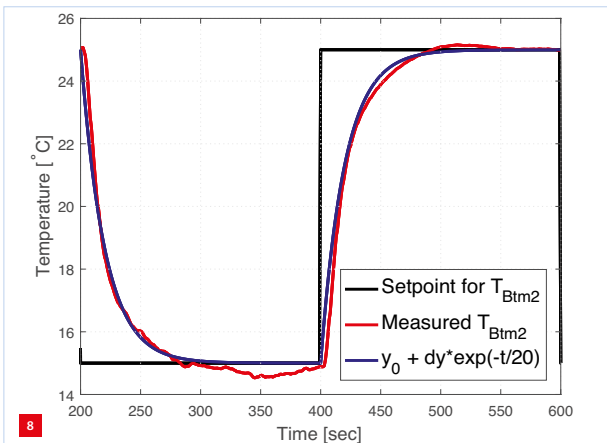
peltier is set to reach its setpoint as fast as possible, accepting the corresponding overshoot, while the second peltier is set to decently converge to the setpoint via a first-order linear response with a time constant of 20 s.

Figure 7 presents the results. As can be seen, the first peltier tries to reach its setpoint as fast as possible after a step in the reference. This results in overshoot (~6%) of the setpoint, which is acceptable. The second peltier converges to its setpoint with a first-order response with $\tau = 20$ s. To emphasise this, Figure 8 shows the response from 200 s to 600 s, together with the first-order response.

Pulsed reference tracking with large dT

Finally, the IO linearising feedback is put to the test by forcing the first peltier to follow a pulsed function with large amplitude, while the second peltier maintains a constant temperature:

$$\begin{aligned} R_1(t) &= 45 + 30 \cdot \text{sign}(\sin(2\pi/1200 \cdot t)) \\ R_2(t) &= 10 \end{aligned} \quad (13)$$



Response of peltier 2 together with a first-order response with $\tau = 20$ s.

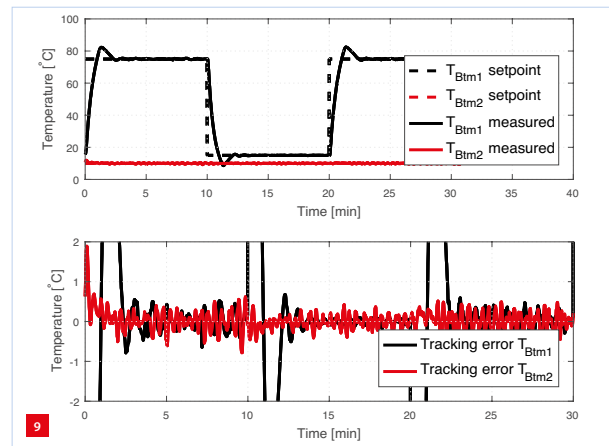
Figure 9 shows the results of this experiment. As can be seen the control law even manages to overcome the 60 K temperature step without any abnormalities. Again the setpoint is reached as fast as possible, considering Peltier limitations. This time it introduces an overshoot of 7 K ($\approx 11\%$), meaning the linear character of the control law is not maintained completely (overshoots should scale linearly). This is the result of modelling inaccuracies, parameter nonlinearities and other nonlinearities in the set-up, such as those in the amplifiers. Nonetheless, the control law is able to stabilise the input-output behaviour.

The bottom of the second peltier must be kept at 10 °C, even during the interference of the evolution of the first peltier. As can be seen, the control law succeeds in this with a tracking error of only 0.4 K. Note that the tracking error is higher in the time frame that the first peltier is at 75 °C because of the increased condensation on the cold peltier next to the hot one.

Conclusions and future work

This study has tested a practically feasible IO linearisation scheme on an experimental set-up with Peltier elements representing a part of a handheld diagnostic device. The added value compared to other studies is in the explicit modelling of effects that degrade the control performance when going from an ideal model to a practical test set-up. For that purpose, a standard IO linearising feedback has been extended with a PI-control law to perform fast and accurate temperature control on two individual Peltier devices that influence each other via thermal connection through a stainless steel bottom plate.

Experimental results show that the adapted IO linearising feedback law is very suitable for the control of Peltier elements in practical applications. Both sinusoidal references as well as pulsed step references can be followed adequately.



Responses of the set-up's bottom plate temperature directly under the peltiers, for temperature setpoints following Equation 13. Top: bottom plate temperatures. Bottom: tracking errors.

Nevertheless, the well-known compromise between settling time and overshoot must be considered in the PI-control law of the IO linearising feedback. The PI-control law does seem stable in the entire application range, however.

In order to further improve the closed-loop performance of this test set-up, the practically feasible control law should be designed to more closely mimic the ideal IO linearisation case. To that end, a nonlinear observer could be implemented in order to estimate the temperature states that cannot be measured. This could potentially eliminate the overshoot during pulsed references.

Currently, research is conducted in cooperation with Eindhoven University of Technology within the framework of the Advanced Thermal Control Consortium.


Ph.D. candidate Enzo Evers and M.Sc. student Rens Slenders, both supervised by associate professor Tom Oomen, are investigating identification techniques to a) better identify the peltier model, b) build an observer for the set-up, and c) quantify the residue nonlinearity after IO linearisation to improve this control law (see also the article on page 12 ff).

Acknowledgements

This study was carried out using the Philips Innovation Services thermal control platform. This platform consists of software developed in-house that enables the real-time use of Matlab Simulink for data acquisition and manipulation of thermal systems. Andre Faesen and Joost Groenen are much appreciated for creating this software.


REFERENCES

- [1] M. Kaya, "Experimental study on active cooling systems used for thermal management of high-power multichip light-emitting diodes", *The Scientific World Journal*, vol. 2014.
- [2] P. Yager, et al., "Microfluidic diagnostic technologies for global public health", *Nature*, vol. 442, 2006.
- [3] J. Jiang, et. al., "Nonlinear controller designs for thermal management in PCR amplification", *IEEE Transactions on Control Systems Technology*, vol. 20, 2012.
- [4] A. Pettes, M. Hodes, and K. Goodson, "Optimized thermoelectric refrigeration in the presence of thermal boundary resistance", *IEEE Transactions on Advanced Packaging*, vol. 32, 2009.
- [5] C. Zhang, et. al. "PCR microfluidic devices for DNA amplification", *Biotech. Adv.*, vol. 24, 2006.
- [6] J. Khandurina, et al., "Integrated system for rapid PCR-based DNA analysis in microfluidic devices", *Analytical Chemistry*, vol. 72, 2000.
- [7] J. Jiang, "Nonlinear controller designs for thermal management in PCR amplification", *IEEE Transactions on Control Systems Technology*, vol. 20, 2012.
- [8] J. Chen, "Thermal controller design for a Lab-on-Chip benchmark", M.Sc. thesis, Eindhoven University of Technology, 2013.
- [9] H. Khalil, *Nonlinear systems*, Prentice Hall, 3rd edition, 2002.
- [10] T. Kailath, *Linear systems*, Prentice Hall, 1st edition, 1980.


FAULHABER

FAULHABER BXT

Power in new dimensions




FAULHABER Brushless Flat DC-Servomotors of the BXT family

- 14-pole external rotor motors with very high continuous torques of up to 134 mNm and powers up to 100W
- Extremely short design with lengths of only 14, 16 and 21 mm, with corresponding diameters of 22, 32 and 42 mm
- Innovative winding technology
- Available with and without housing

www.faulhaber.com/p/bxt/en

NEW



WE CREATE MOTION

Accelerating quickly depends mostly on shifting fast and well

Developing, creating, assembling and testing complex (opto)mechatronic systems and mechanical modules is just like taking part in a Formula 1 race. Everything revolves around precision and maneuverability, NTS knows that better than anyone. We have gathered a lot of knowledge and know-how of systems and modules for handling, transfer and positioning in machines. We apply our knowledge and competences in various fields worldwide to our clients' unique products: high-tech machine builders (OEMs).

In this way, they can focus on their core processes and also deliver machines with a shorter lead time, at lower costs. We are flexible and ambitious and keep the engine running, for the entire lifecycle. We step on the gas, and lose as few rpm's as possible. Fast and good. That's how you stay ahead. With the energy that is released, our clients accelerate in their business pursuits. Do you also want to accelerate and shift faster with NTS? Our engine is heating up to get to know you better.

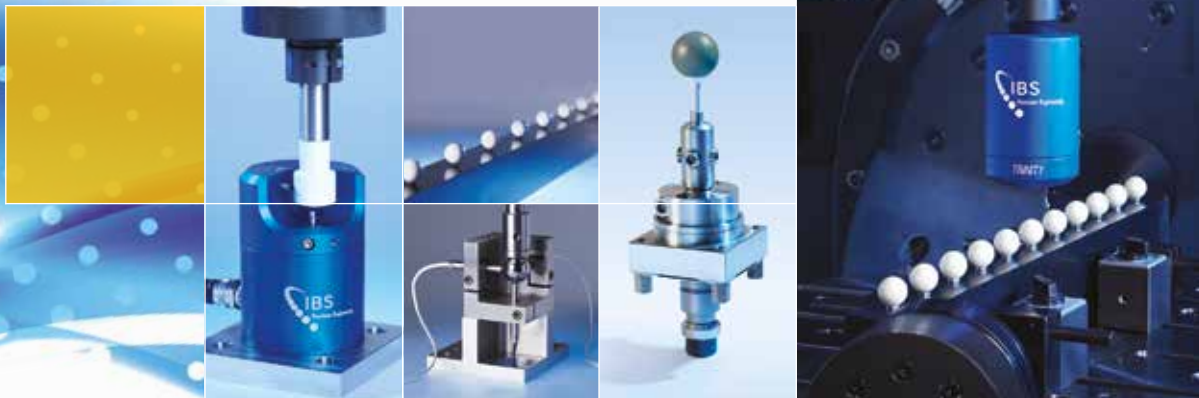
www.nts-group.nl

Accelerating your business



Machine Tool Qualification

Linear axis, rotary table & spindle accuracy



www.ibspe.com

CHALLENGES AND OPPORTUNITIES FOR SYSTEM IDENTIFICATION

Thermal effects are becoming increasingly important in efforts to enhance the performance of electron microscopes. Therefore, accurate thermal-mechanical models are desired for analysis and control. Modelling thermal systems from experimental data, i.e. system identification, is challenging due to large transients, large time scales, excitation signal limitations, large environmental disturbances, and nonlinear behaviour. An identification framework has been developed to address these issues. The presented approach facilitates the implementation of advanced control techniques and error compensation strategies by providing high-fidelity models.

ENZO EVERS, RONALD LAMERS AND TOM OOMEN

Introduction

Thermo Fisher is a leading manufacturer of electron microscopes. Their high-end (transmission) electron microscopes are developed and produced in Eindhoven (NL). These systems are capable of visualising objects at the atomic scale with a resolution down to 50 picometer (sub-Ångström resolutions).

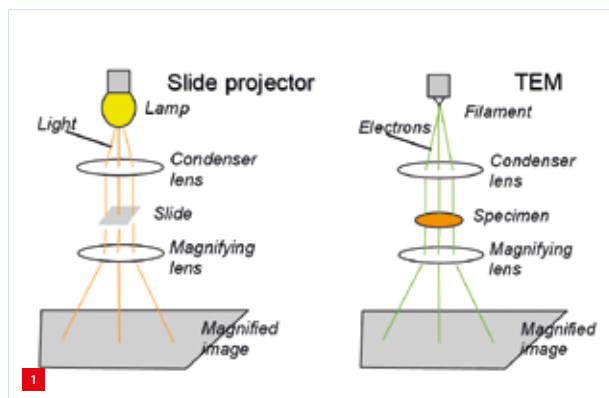
The goal of an electron microscope is to acquire high-quality and high-resolution images of a specimen. The basic operation principle of an electron microscope, which is similar to that of a conventional light microscope or slide projector, is shown in Figure 1. Whereas a slide projector works with light and optical lenses, an electron microscope works with electrons and electromagnetic lenses.

A general overview of a transmission electron microscope is shown in Figure 2. The electron beam is generated inside the electron source, and the electrons pass through the condenser lens system, which makes the electron beam parallel. Then, the electron beam passes through a thin specimen that is mounted on a sample manipulation stage. This stage can move the specimen with respect to the electron beam, hence a large area of the specimen can be imaged. The corrector lens system is an additional module that can be placed on the electron microscope to correct for optical aberrations. Finally, the projector lens system magnifies the image and projects it onto a camera.

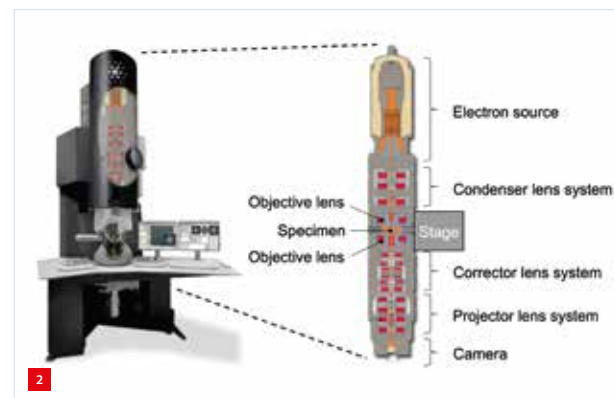
AUTHORS' NOTE

Enzo Evers (Ph.D. candidate) and Tom Oomen (associate professor) are both associated with the Control Systems Technology group within the department of Mechanical Engineering at Eindhoven University of Technology in Eindhoven (NL). Ronald Lamers works as a thermal dynamic design engineer at Thermo Fisher in Eindhoven. The authors gratefully acknowledge Niels van Tuijl for his contribution to this work.

e.evers@tue.nl
www.tue.nl/cst
www.thermofisher.com
www.toomen.eu



Similar operation principle of a slide projector and a transmission electron microscope (TEM) [1].



General overview of a transmission electron microscope [2].

Advanced Thermal Control Consortium

Thermo Fisher has joined the Advanced Thermal Control Consortium. The aim of this consortium is to advance the theoretical and applied approaches to design, simulation, measurement and compensation techniques essential for the development of precision modules/systems subject to internal or external thermal loads [3]. Within this consortium, a fruitful collaboration between Thermo Fisher and Eindhoven University of Technology has been set-up to expand the identification and control approaches available for thermal-mechanical systems.



WWW.TUE.NL/HTSC

Because an electron microscope is capable of visualising objects at the atomic scale, it is a key enabler for nanotechnology, life science, material science and semiconductor technology. Electron microscopes are increasingly being used as analysis tools in laboratories and industry. Whereas the material science market is pushing the boundaries with respect to resolution of electron microscopes, markets as semiconductors and life science are pushing the boundaries with respect to throughput. In view of these increasing demands for throughput and resolution, the stability of electron microscopes becomes increasingly important.

Stability

Acquiring high-resolution images requires the exposure time of the camera to be sufficient long. The image acquisition process takes time, because a sufficient amount of electrons need to be detected in order to provide enough contrast in an image, which is the main measure for image quality. In fact, the contrast improves with increased exposure time. During the exposure time, the specimen

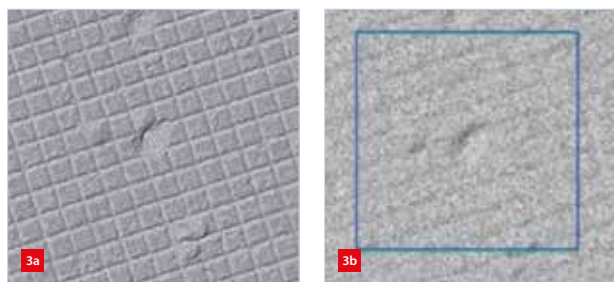


Image of an object (gold) [4].
(a) In high contrast.
(b) With blur.

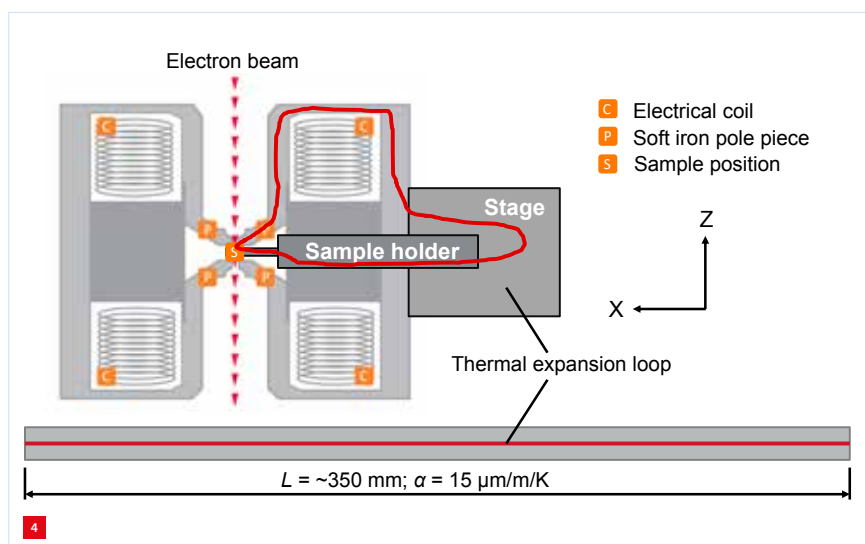
must remain stationary with respect to the electron beam. Movement of the specimen, known as drift, would lead to a blurred image, as shown in Figure 3. In this context, stability is defined as minimal drift of the sample position with respect to the electron beam. At present, the state-of-the-art approach is to wait (minutes to hours) until the drift is low enough for high-quality imaging, which significantly reduces the throughput of the system.

For example, in life science applications a so-called single-particle analysis is performed to study single proteins that perform key roles in diseases in their native context in the cell at near atomic resolution. In such analyses, the microscope can be taking images automatically for several days, during which image quality, and thus stability ($< 10 \text{ nm/min}$) of the electron microscope must be guaranteed.

Sensitivity

In Figure 4, a more detailed view is given on the specimen location inside the electron microscope. The specimen is placed on a sample holder, which will be positioned inside the sample manipulation stage and the electron microscope. Also shown in Figure 4 is the thermal expansion loop.

The thermal expansion loop covers parts of the electron microscope on which the stage has been mounted, parts of the stage, and parts of the sample holder. If the temperature of these parts changes due to thermal disturbances, they will deform, which will cause drift of the sample position with respect to the electron beam. The thermally induced deformation in X-direction is far more dominant than in Z- and Y-direction, therefore the thermal expansion loop can be considered as a sum of 1D expansions in X-direction of all parts inside the loop. The maximum allowed drift of the specimen is 0.5 nm/min .



Main drift components and expansion loop.

For an impression of the required temperature stability, the thermal expansion loop is folded open; the total length is approximately 350 mm. If an average coefficient of thermal expansion is assumed for all the parts of $15 \mu\text{m/m/K}$, the required temperature stability of the thermal expansion loop to meet the drift requirement of 0.5 nm/min is 0.1 mK/min . This temperature stability requirement is worst-case, since thermal expansions can cancel each other. However, the coefficients of thermal expansion and thermal time constants differ for all parts inside the expansion loop.

Main disturbances

The performance of electron microscopes is disturbed by mechanical vibrations and acoustics, and electromagnetic fields, but also due to thermal disturbances. These cause thermal-mechanical deformations of the system, which are observed in the image as drift. Thermal disturbances can be divided in external and internal disturbances. Main external disturbances are the air temperature variations in the electron microscope room and the temperature and flow variations of the cooling water. Main internal disturbances are temperature variations due to power dissipation variations of the electromagnetic lenses, motors and encoders.

A special case of disturbance is the insertion of a specimen holder. Typically, the temperature of the sample holder is not equal to that of the microscope. The sample holder has to take over the temperature of the microscope, and until a new thermal equilibrium is reached, the system will be subject to drift.

For counteracting acoustic disturbances high-end electron microscopes are placed in an acoustic enclosure, as shown in Figure 5. This acoustic enclosure also attenuates the effect

of room temperature variations. The thermal time constant of such an enclosure is approximately 4 hours. This means that slow room air temperature variations, such as the day-night cycle, are still affecting the electron microscope, leading to thermally induced drift of the sample position with respect to the electron beam.

Power dissipation inside the sample manipulation stage due to motors and encoders, albeit only a few milliwatts, causes drift. The power dissipation of the electromagnetic lenses is also a main thermal disturbance. Although most electromagnetic lenses are operated in a constant-power setting, this is not applicable for all lenses inside the electron microscope. So, the variation in the power dissipation of the electromagnetic lenses is also a source of drift.

System identification

To meet the ever-increasing demands to enhance the throughput and positioning accuracy, thermal deformations must be analysed and compensated for using real-time error compensation techniques and an appropriate thermo-mechanical model. Accurate modelling of precise thermo-mechanical systems is complex, e.g., due to uncertain parameters and contact resistances. Earlier solutions to compensate for the deformations in electron microscopes, for instance, cannot cope with large deformations and strongly depend on model quality [5] [6]. Therefore, an accurate parametric model is desired for a model-based approach. Ideally, using a limited amount of temperature measurements combined with an accurate thermo-mechanical model enables the deployment of error-compensation techniques [7] [8].

State-of-the-art at Thermo Fisher

The state-of-the-art for thermal-mechanical system identification within Thermo Fisher is to apply step-like heat load excitations, and measure the response in temperature and/or drift. In certain scenarios, e.g., for measuring cooling-water-related transfer functions, a square-wave waveform is used as input signal, with a duty cycle of 50%, in which the time period of the waveform is varying.

Models are tuned (as yet) manually based upon the measured data in the time and frequency domain. The time constants of the system can be as long as 12 hours. Especially long time constants often result in experiments, either in the time or frequency domain, running for multiple days. During these measurements, the experiment is influenced by disturbances, including the varying ambient temperature. These influences often lead to poor signal-to-noise ratios, so that the information obtained from the experiment is limited.



Thermo Fisher Titan microscope outside an opened acoustic enclosure.
(Photo: Leo Koomen)

Currently, experimental modelling of thermal systems is often done by sequential excitation of system inputs until steady state is achieved. Due to the large time constants in thermal systems, this method rapidly becomes tedious for an increasing number of inputs. There is a strong desire to reduce the time and to improve the quality of the measurements, and to improve the estimation of uncertain model parameters, such as the emissivity in radiation heat transfer, thermal contact resistances and material properties, e.g. at cryogenic temperatures.

Advances

Here, the key contribution lies in accurate modelling of thermomechanical behaviour using multi-input multi-output (MIMO) frequency response function (FRF) identification. Advances in system identification are leveraged to model thermomechanical systems and yield improved system models [9]. The approach is threefold and comprises the following contributions:

- Fast and accurate multivariable FRF estimations of thermal systems under transient conditions.
- Improved low-frequency estimation error by incorporation of additional sensor inputs.
- Estimation of thermal system parameters using a grey-box approach.

Transients

Consider a causal linear discrete time-invariant (LTI) system in an open-loop identification setting. The response $y(n)$ to an input $u(n)$ is given by:

$$y(n) = \sum_{m=-\infty}^{\infty} g(n-m)u(m)$$

Here, $g(n)$ is the impulse response of the system. Taking a measurement from t_{start} to t_{end} of length N and applying the discrete Fourier transform (DFT) yields:

$$Y(k) = G(\Omega_k)U(k) + T(\Omega_k)$$

Here, $\Omega_k = e^{-\frac{i2\pi k}{N}}$ with N the number of samples and $Y(k)$ and $U(k)$ the DFT of $y(m)$ and $u(m)$, respectively, and $G(\Omega_k)$ the frequency response function of the LTI system. Additionally, a term $T(\Omega_k)$ is required to account for the transient response by going from infinite time to a discrete time interval.

Traditionally, the empirical transfer function estimation (ETFE) is used to derive the FRF, defined as:

$$\begin{aligned}\hat{G}_{etfe}(\Omega_k) &= Y(k)U(k)^{-1} \\ &= G(\Omega_k) + T(\Omega_k)U(k)^{-1}\end{aligned}$$

Here, $T(\Omega_k)U(k)^{-1}$ is an estimation bias of the ETFE caused by transients in the response $y(n)$. While the ETFE can often yield acceptable results on mechanical systems, since

the transient is significantly shorter than the measurement period, for thermal systems the estimation accuracy is severely biased due to the strong transients and large time constants, e.g. 4 hours for the acoustic enclosure. To reduce the estimation error, the transient should be explicitly addressed during the FRF estimation.

Local parametric modelling

To cope with data gathered under transient conditions, a local modelling method is adopted. The method is developed in [10] and applied in [11] and it uses a local rational parameterisation of $G(\Omega_k)$ and $T(\Omega_k)$. The system dynamics and transient are parametrised for a small local frequency window $k+r$ as:

$$\begin{aligned}G(\Omega_k) &= \sum_{b=0}^{N_b} \theta_G B_b(k+r) \\ T(\Omega_k) &= \sum_{b=0}^{N_b} \theta_T B_b(k+r)\end{aligned}$$

Here, B_b are the basis functions and θ the corresponding estimation parameters. This parametrisation is linear in the parameters, i.e. the optimisation is convex with an analytic solution. Moreover, the basis functions B_b are user-specified, e.g. orthonormal rational functions. This combines the benefits of a linear optimisation and a rich, possibly rational, parameterisation. By explicitly estimating the transient term $T(\Omega_k)$ it can be removed from the FRF estimation of $G(\Omega_k)$, thus avoiding the estimation bias that would be obtained using the ETFE. Moreover, since transient data can be used, which is otherwise often discarded, a significant reduction in experimental measurement time is achieved.

Incorporating additional sensor inputs

One of the main environmental disturbances are the fluctuations in ambient temperature. To reduce the effect of these disturbances on the system identification set-up, measurements of the ambient temperature are incorporated as an additional input. In particular:

$$Y(\Omega_k) = \hat{G}(\Omega_k) \begin{bmatrix} U(k) \\ D(k) \end{bmatrix} + T(\Omega_k)$$

Here, $D(k)$ is the DFT of the measured environmental disturbance, e.g. the ambient temperature. Here, $\hat{G}(\Omega_k)$ is now a 1x2 multi-variable transfer function matrix since it includes an additional transfer function, i.e. $\hat{G}(\Omega_k) = [G(\Omega_k)_{u_1 \rightarrow T_1} \quad G(\Omega_k)_{T_{\infty} \rightarrow T_1}]$. By using the proposed local parametric method, this full transfer function matrix is estimated from the measurement data. Since the ambient temperature typically contains the most energy at lower frequencies, including this as an additional 'excitation' input removes a low-frequency disturbance and consequently leads to improved estimation results for this frequency range.

Parameter estimation

A lumped-parameter model is often used for initial analysis during the design process, and initial prototyping stage. To facilitate model-based control and error compensation approaches, an accurate parametric model of the thermo-mechanical system is desired. The lumped-parameter model often contains parameters and boundary conditions that are uncertain or unknown, e.g. material properties or thermal contact resistances. At present, models are tuned manually based upon the measured data in the time and frequency domain. With increasing complexity of the physical systems, and their corresponding models, the manual tuning of parameters is becoming too cumbersome.

Grey-box identification

To yield high-fidelity thermomechanical models, grey-box identification is used to improve the accuracy of unknown parameters in the lumped-parameter models. By means of spatial discretisation of the thermal dynamics a parameterised model is generated, here shown in state-space form:

$$G(\Omega_k, \phi) := \begin{cases} T(t) = A(\phi)T(t) + B(\phi)u(t) \\ y(t) = C(\phi)T(t) \end{cases}$$

Here, $\phi \in R^{N_p \times 1}$ is the parameter set with N_p the number of parameters. The aim of grey-box identification is to calibrate the parameter set ϕ such that the model is suitable for control. The approach is based on minimising the discrepancy between the measured non-parametric FRF and the FRF of the parametric model with the following cost function:

$$J(\phi) = \min_{\phi} \left\{ \left\| W(\Omega_k) \left(\hat{G}(\Omega_k) - G(\Omega_k, \phi) \right) \right\|_2^2 \right\}$$

Here, $\hat{G}(\Omega_k)$ is the measured FRF, $G(\Omega_k, \phi) = C(\phi)(\Omega_k - A(\phi))^{-1}B(\phi)$ is the FRF of the parametric model and $W(\Omega_k)$ is a dynamic weighting filter based on the variance of the measured FRF. By minimising the cost function J the parameter values in ϕ become such that the parametric model best describes the experimental system. This yields a high-fidelity model suitable for advanced control and error compensation techniques.

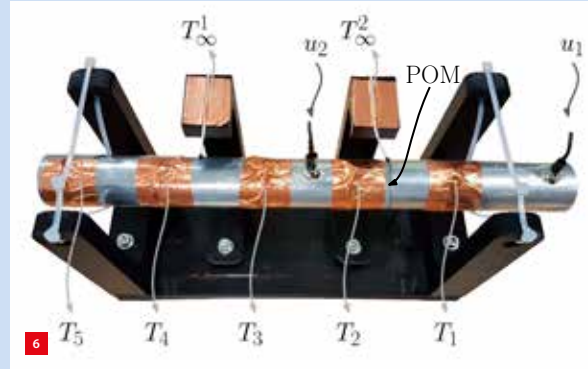
Case study

The presented approaches for system identification are applied to a 1D thermal system; see the box on the right.

(Main article continued on page 18.)

Case study: 1D thermal system

The experimental set-up shown in Figure 6 consists of an aluminium cylinder containing a slice of high-thermal-resistance material (POM), two excitation inputs (u_1, u_2), two temperature sensors ($T_i, i \in [1,5]$) and two ambient temperature sensors (T_{∞}). The experimental set-up is representative of a chain of thermal resistances in 1D, a situation commonly found in electron microscopes where the thermal expansion is considered dominant in one direction; see, e.g., Figure 4.



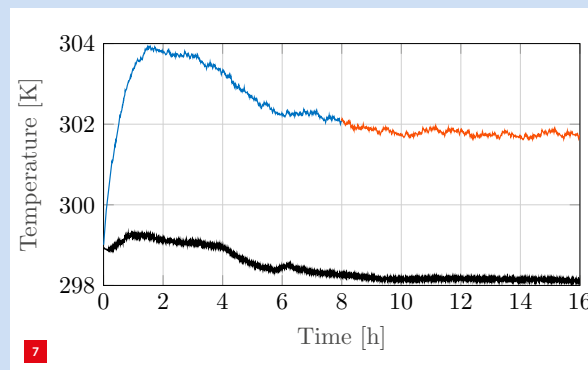
Experimental set-up. An aluminium cylinder containing a slice of high-thermal-resistance material (POM), two excitation inputs (u_1, u_2), two temperature sensors ($T_i, i \in [1,5]$) and two ambient temperature sensors (T_{∞}).

Identification under transient conditions

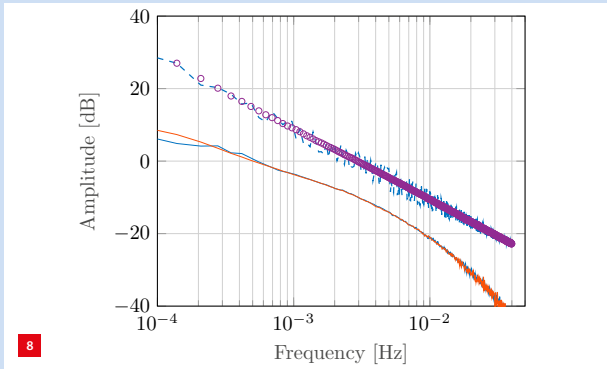
The local parametric method has the potential to construct a system FRF from data obtained under transient conditions. For this, the heater u_1 and sensor T_1 , shown in Figure 6, are used as input and output, respectively. The excitation signal $u_1(t)$ is a random-phase multi-sine, i.e. a collection of sinusoidal signals:

$$u_1(t) = \sum_{k=1}^N A_k \sin\left(\frac{2\pi kt}{N} + \psi_k\right) + \Delta$$

Here, N is the amount of samples in one period, A_k is an amplitude, ψ_k a uniformly distributed phase on $[0, 2\pi)$ and Δ an off-set since the input is constrained to be positive. By then applying 4 periods of each 4 hours as excitation, a time-domain response as shown in Figure 7 is obtained.



Temperature response $u_1 \rightarrow T_1$ of the experimental set-up to a random-phase multi-sine with offset for 4 periods of each 4 hours. The dataset is divided into two sub-records, (1) containing the first two periods (in blue), and (2) containing the last two periods (in red), considered as a validation data-set. A measurement of the ambient temperature T_{∞} is shown in black.



FRF estimation using the ETFE (blue dashed) and the proposed method (blue solid). It shows that the ETFE clearly estimates an erroneous FRF when compared to the validation data (red solid), while the proposed method does not. This is caused by the transient component $T(O_k)$, indicated as magenta circles.

The time-domain response shows an initial step-like response in temperature, due to the offset Δ in u_1 , in addition to a periodic response to the multi-sine excitation.

Two sub-records of the same dataset are considered:

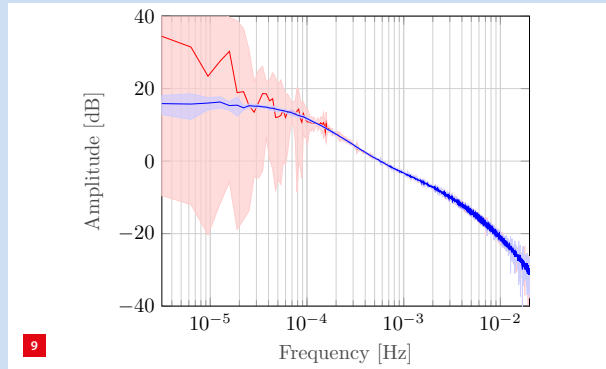
- The first sub-record includes the first two periods, containing a significant initial transient and environmental disturbances.
- The second sub-record consist of the last two periods with a substantially smaller transient and environmental disturbance, and is used as a validation dataset.

Applying both the proposed local parametric identification method and the ETFE on the first sub-record of the data in Figure 7 yields results as shown in Figure 8. Both methods are compared to the FRF obtained by applying the proposed method on the second sub-record, which is considered a validation dataset. It then shows that the ETFE is severely biased by the transient component $T(O_k)$, shown as magenta circles, while the proposed method is not.

This illustrates that the proposed method is insensitive to the initial transient in the data set and estimates an FRF that is almost identical to the one obtained from the validation record. This potentially leads to significant savings in experimental time, since now data obtained under transient conditions can be used that would otherwise be discarded.

Incorporating additional inputs

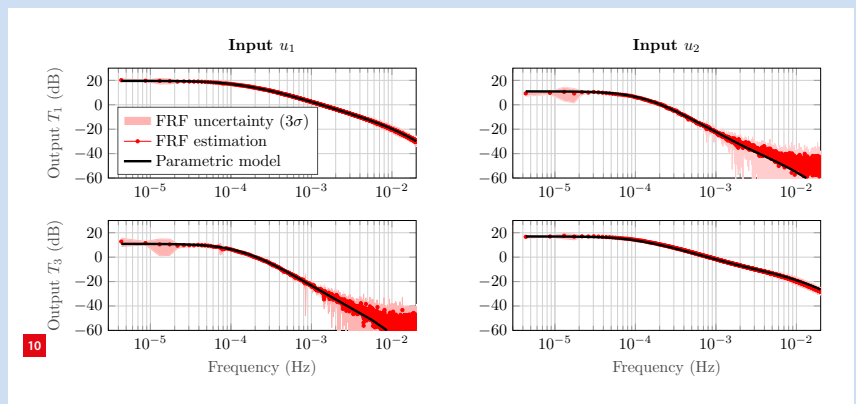
Incorporating additional input signals can potentially yield an improved FRF estimation by increasing the energy in the system. The results in Figure 9 illustrate effects of including the ambient temperature T_∞ as an additional input. It shows that the low-frequency estimation is improved and a smaller variance is achieved, as indicated by the shaded area.



FRF estimation of $u_1 \rightarrow T_1$ by (a) using only input u_1 (red); and (b) incorporating additional inputs (blue), thereby reducing the impact of environmental disturbances on the FRF estimation. This results in an improved low-frequency FRF estimation, since these disturbances typically contain most of their energy in this region.

Grey-box parameter estimation

The cumulative effort of the previous techniques yields an accurate FRF suitable for parameter calibration. The parameters of a multi-input multi-output (MIMO) lumped-capacity thermal model are calibrated by minimising the cost function $J(\theta)$ using a Nonlinear Least Squares optimisation procedure in MATLAB. In Figure 10 the estimated non-parametric FRF and the calibrated parametric model are shown. Clearly, the estimated parametric model is within the 3σ uncertainty of the FRF estimation.



Non-parametric FRF estimate (dotted) of the experimental set-up and the 3σ estimation uncertainty (red shaded). The FRF is used for a grey-box parameter estimation, yielding a high-fidelity parametric model (black solid)

Moreover, it shows that the transfer functions on the off-diagonal have a reduced gain level and an increased estimation uncertainty. This is the result of the slice of POM material glued in between the two aluminium parts of the beam, as shown in Figure 6. The POM material has a lower conductivity, therefore acting as a high thermal resistance between $u_1 \rightarrow T_3$ and $u_2 \rightarrow T_1$ making the identification of the related transfer functions increasingly difficult due to the reduced signal-to-noise ratio. The proposed calibration procedure yields a MIMO high-fidelity parametric model of the experimental system that is suitable for advanced control techniques and error compensation strategies that enable increased attenuation of thermal-induced deformation errors.

Summary

Drift caused by thermal expansion in an electron microscope is one of the leading sources of error in the final imaging performance. Moreover, due to the ever-increasing demands to enhance the throughput and positioning accuracy, the specifications for the drift requirements are increasingly stringent. This necessitates a thorough analysis of the thermal effects and an appropriate control approach using an accurate thermomechanical model. Accurate modelling of precise thermomechanical systems is complex, e.g., due to uncertain parameters and contact resistances.

The identification framework presented in this article enables the fast and accurate identification of thermal dynamics in view of precision motion control. The proposed methodology has been applied to a multi-variable experimental set-up. It achieved a significant improvement in estimation accuracy and a reduced experimentation time by suppressing the transient and disturbance contributions. The presented methods facilitate the implementation of advanced control techniques and error compensation strategies, enabling increased accuracy and throughput in electron microscopy and other high-precision mechatronic systems.

REFERENCES

- [1] TEM intro for Non-Technical employees ILT, Thermo Fisher internal course.
- [2] "An introduction to electron microscopy", www.fei.com/WorkArea/DownloadAsset.aspx?id=15032385923
- [3] D.T. Spaan-Burke, "Advanced Thermal Control Consortium", www.ibspe.com/public/uploads/content/files/ATCTier%203%20Flier%20Aug%202016.pdf
- [4] E. van Horssen, "Data-intensive feedback control: switched systems analysis and design", Ph.D. thesis, Eindhoven University of Technology, 2018.
- [5] B.S. Salmons, D.R. Katz and M. L. Trawick, "Correction of distortion due to thermal drift in scanning probe microscopy", *Ultramicroscopy*, vol. 110, no. 4, pp. 339-349, 2010.
- [6] A.N. Tarau, P. Nuij and M. Steinbuch, "Hierarchical control for drift correction in transmission electron microscopes", in *2011 IEEE International Conference on Control Applications (CCA)*, Denver, CO, USA, 2011.
- [7] E. Evers, M. van de Wal and T. Oomen, "Synchronizing decentralized control loops for overall performance enhancement: A youla framework applied to a wafer scanner", in *20th IFAC World Congress*, Toulouse, France, 2017.
- [8] A.H. Koevoets, H.J. Eggink, J. van der Sanden, J. Dekkers and T.A.M. Ruijl, "Optimal sensor configuring techniques for the compensation of thermo-elastic deformations in high-precision systems", in *13th International Workshop on Thermal Investigation of ICs and Systems (THERMINIC)*, 2007.
- [9] E. Evers, N. van Tuijl, R. Lamers and T. Oomen, "Identifying Thermal Dynamics for Precision Motion Control", submitted for conference publication, 2019.
- [10] E. Evers, B. de Jager and T. Oomen, "Improved local rational method by incorporating system knowledge: with application to mechanical and thermal dynamical systems", in *18th IFAC symposium on system identification*, Stockholm, 2018.
- [11] E. Evers, B. de Jager and T. Oomen, "Thermo-Mechanical Behavior in Precision Motion Control: Unified Framework for Fast and Accurate FRF Identification", in *IECON 2018 - 44th Annual Conference of the IEEE Industrial Electronics Society*, Washington, DC, USA, 2018.



Application Engineer PECM (Research Instrument maker PECM)

Do you have the drive to always develop yourself, and also the process you're working with?
Are you looking for an independent job where you are in the lead with the development of the technical possibilities of our PECM machine? And are you looking to apply this technology on new and existing products?

Job features:

- Assembly of tools and preparation of PECM machine
- Handling and alignment of tooling
- Problem-solving, debugging and securing this knowledge
- Making of prototypes and documenting the results.
- Making adjustments to the tooling if necessary, to achieve a good result.

Do you see yourself working at a High-Tech family company with approx. 40 colleagues located in the East of the Netherlands? If yes, then you could become our new colleague Application Engineer PECM.

If you want more information about this exciting job offer, please contact our colleague from HR:

Annelien Weenink (annelien@terhoek.com).

Or visit our website (www.terhoek.com).

UPCOMING EVENTS

7 May 2019, Veldhoven (NL) Laser & Photonics Event

Event, organised by Mikrocentrum, dedicated to imaging/sensor technology, (optical) test and measurement systems for the manufacturing industry, lasers and laser systems for production applications, and optics manufacturing.

WWW.PHOTONICS-EVENT.NL

15 May 2019, Den Bosch (NL) National Contamination Control Symposium

Event, organised by VCCN, comprises a lecture programme, tutorials and an exhibition. One of the sessions is devoted to smart(er) cleanrooms.



WWW.VCCN.NL

15-16 May 2019, Leuven (BE) Materials+Eurofinish 2019

At this joint event material science meets surface technology. Combined, these ingredients help to achieve sustainable designs and innovative ideas, from (new) materials, material analysis and surface technology to binding techniques. The fair provides a complete overview of the entire value chain: from raw materials to a finished product.

WWW.MATERIALS.NL

23 May 2019, Eindhoven (NL) Precision-in-Business Day

DSPE event hosted by NTS, first-tier systems supplier in optomechatronic systems and mechanical modules for large, high-tech OEMs. See also page 46.

WWW.DSPE.NL/EVENTS/PIB-EVENTS

3-7 June 2019, Bilbao (ES) Euspen's 19th International Conference & Exhibition

This event features latest advances in traditional precision engineering fields such as metrology, ultra-precision machining, additive and replication processes, precision mechatronic systems & control and precision cutting processes. Furthermore, topics will be

addressed covering robotics and automation, Industrie 4.0 for precision manufacturing, precision design in large-scale applications and applications of precision engineering in biomedical sciences.

WWW.EUSPEN.EU

6 June 2019, Enschede (NL) TValley Annual Congress 2019

The congress will provide a state-of-the-art overview of robotics and mechatronics R&D activities of the TValley network and its industrial partners. The Tvalley agenda includes mechatronics education, knowledge exchange, specific projects on robotics and smart industry, and profiling of the high-tech industry in the east of the Netherlands.



WWW.TVALLEY.NL

12-13 June 2019, Veldhoven (NL) Vision, Robotics & Motion 2019

This trade fair & congress presents the future of human-robot collaboration within the manufacturing industry.

WWW.VISION-ROBOTICS.NL

20 June 2019, Den Bosch (NL) Dutch System Architecting Conference

The second edition of this conference features system architecting as a distinguishing discipline in the development and commercialisation of complex systems, products and machines.

WWW.SYSARCH.NL

25-27 June 2019, Erfurt (DE) Rapid.Tech + FabCon 3.D

International trade show and conference for additive manufacturing.

WWW.RAPIDTECH-FABCON.DE

27 June 2019, Eindhoven (NL) DSPE Knowledge Day

DSPE event on Engineering for Particle Contamination Control. See also page 46.

WWW.DSPE.NL/EVENTS/AGENDA

16-18 September 2019, Nantes (FR) SIG Meeting Advancing Precision in Additive Manufacturing

Special Interest Group Meeting hosted by euspen (European Society for Precision Engineering and Nanotechnology) in collaboration with ASPE (American Society for Precision Engineering). This year's SIG will focus on, a.o., dimensional accuracy and surface finish from AM, design for precision, standardisation, metrology, and integration of AM into an overall holistic manufacturing process.

WWW.EUSPEN.EU

8-10 October 2019, Karlsruhe (GE) DeburringEXPO

Third edition of trade fair for deburring technology and precision surface finishing.



WWW.DEBURRING-EXPO.COM

28 October - 1 November 2019, Pittsburgh (PA, USA)

34th ASPE Annual Meeting

Meeting of the American Society for Precision Engineering, introducing new concepts, processes, equipment, and products while highlighting recent advances in precision measurement, design, control, and fabrication.

WWW.ASPE.NET

13-14 November 2019, Veldhoven (NL) Precision Fair 2019

Nineteenth edition of the Benelux premier trade fair and conference on precision engineering, organised by Mikrocentrum.

WWW.PRECISIEBEURS.NL

27-28 November 2019, Berlin (DE) SIG Meeting Micro/Nano Manufacturing

Special Interest Group Meeting hosted by euspen, focusing on novel methodological developments in micro- and nano-scale manufacturing, i.e. on novel process chains including process optimisation, quality assurance approaches and metrology.

WWW.EUSPEN.EU

THERMAL QUALIFICATION OF PRECISION SYSTEMS

Thermal qualification of a temperature-conditioned heat shield for a precision motion system has been performed using modelling and measurement tools at MI-Partners. Thermal qualification enables determination of thermal system performance without stringent demands on environmental conditions. It combines frequency-domain modelling techniques with measurements on a real system in order to quantify thermal performance. It has been shown to be an effective tool, enabling simple but accurate approval of thermal systems.

MAURICE LIMPENS, BJÖRN BUKKEMS AND THEO RUIJL

Introduction

In precision motion systems where positioning accuracy is of vital importance, thermal effects can lead to significant loss in performance or system failure. Heat sources in the system like actuators and sensors lead to temperature gradients, causing material stress and deformation. Temperature gradients are dependent on the design of the system. In addition to a decent thermomechanical design, such systems often demand specific environmental conditions in order to enable high-precision performance, such as a temperature-stable vacuum environment.

In the design phase, relevant experience and dedicated analysis provide guidelines for a design in order to meet narrow specifications. After the design phase, the specifications need to be proven on actual hardware. Typically, direct measurement of narrow specifications can only be performed under operational conditions. These conditions may not be available or expensive to realise. The method of thermal qualification described in this paper enables testing precise thermal performance of systems and parts without demanding narrow specifications on environmental conditions.

Temperature-conditioned shield

The system considered here is the temperature-conditioned shield shown in Figure 1. The shield is meant to block environmental thermal disturbances under vacuum conditions in a precision motion system. Thermal performance of the shield is quantified by the temperature change of the shield itself while blocking disturbances from the environment. The lower the temperature changes of the shield, the better its thermal performance. The specification on thermal performance for the shield is a maximum deviation of the shield temperature of ± 60 mK for environmental disturbances of ± 1 °C.

The shield is made of aluminium, and has a stainless steel cooling channel glued to its surface. A water flow with precisely controlled supply temperature will be used to condition the shield temperature. Better thermal coupling between the water and the shield will result in reduced effect of environmental disturbances on the shield temperature, which means better thermal performance. To ensure sufficient thermal contact between the plate and the cooling channel, the glue layer is designed to be as thin as possible. Deviation in glue layer thickness, which could possibly occur during assembly, is regarded as a major risk for reduced thermal performance.

Thermal qualification

Directly measuring the specification on thermal performance of the shield would require a vacuum environment under operational thermal conditions. At the location and time of production of the shield,



Water-cooled shield with connected water hoses. The Local Fluid Stream Heater used for thermal qualification is visible in the lower left corner.

AUTHORS' NOTE

The authors are all associated with MI-Partners in Eindhoven (NL), Maurice Limpens as a senior thermal architect, Björn Bukkems as a senior mechatronic system designer and Theo Ruijl as CTO. The latter initiated the TEMS (Thermal Effects in Mechatronic Systems) competence within Philips Applied Technologies about 15 years ago.

maurice.limpens@mi-partners.nl
www.mi-partners.nl

such an environment is not available. However, thermal performance under operational conditions is determined by the thermal behaviour of the shield. This thermal behaviour can also be measured under non-operational conditions.

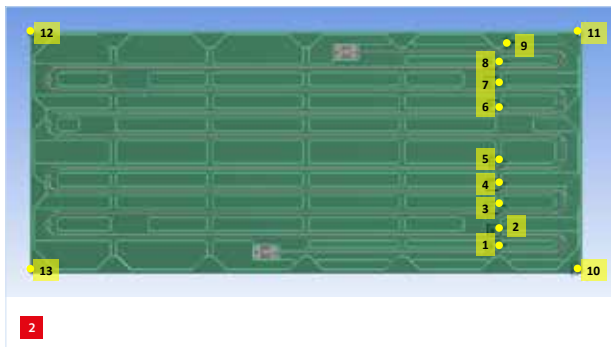
Thermal behaviour is characterised by temperature responses in the shield resulting from fluctuations in cooling water temperature. These thermal responses are a measure for thermal behaviour of the shield, which is influenced by design and manufacturing parameters. Based on the design of the plate, expected thermal responses from fluctuations in cooling water temperature are determined by numerical analysis (FEM). By measuring the responses of the real plate, measured responses can be compared to expected responses from numerical analysis. This will show whether thermal behaviour of the real plate is as expected by design, and whether the plate can be approved or not.

Thermal responses are determined for selected locations on the shield, which are also the sensor positions for thermal measurements. For the shield under consideration, thermal performance specifications are on surface temperatures of the shield. Therefore, sensor positions are all chosen on the shield surface. Thermal resistances that may have significant uncertainty are heat transfer between cooling water and channel wall and thermal conduction of the glue layer. These thermal resistances are in between the cooling water and the sensor positions.

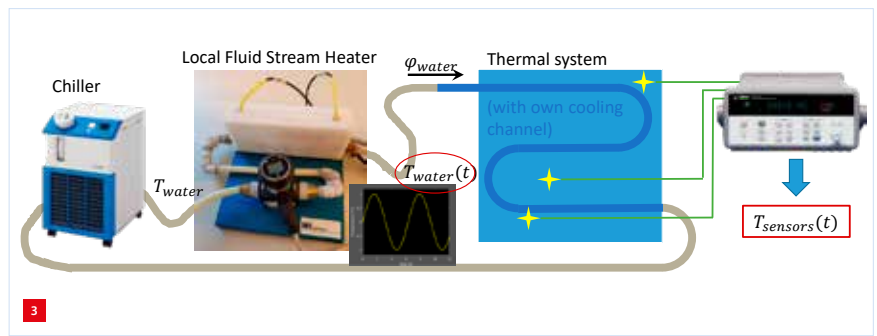
Therefore, quantified thermal responses are dependent on these uncertain thermal resistances. The sensor positions are shown in Figure 2. Most locations are near the cooling channel, as a series along the downstream path of the water. The four corner locations of the shield are also taken into account. Significantly different thermal responses are expected for these corner locations because they are the furthest away from the cooling channel.

Cooling water temperature fluctuation

In order to determine thermal responses on the shield, a sinusoidal temperature fluctuation will be forced on the cooling water. This is possible using the Local Fluid Stream



Top view of the shield with sensor locations indicated by yellow labels.



Global set-up of a thermal qualification measurement. The chiller provides cooling water on a stable base level. The Local Fluid Stream Heater is then used to provide a sinusoidal water temperature fluctuation in the flow towards the plate. Thermal responses at the sensor positions on the plate are measured using temperature sensors on the plate and a data-logger.

Heater, which is a device developed at MI-Partners for obtaining cooling water flow with milli-Kelvin temperature stability that can also be used for performing thermal qualification measurements. The Local Fluid Stream Heater can force a user-defined sinusoidal temperature fluctuation on the supply cooling water flow towards the shield. Thermal responses of the shield can be measured by the temperature sensors enabling characterisation of the shield's thermal behaviour.

Measurement

The experiment is a thermal qualification measurement, for which all necessary equipment is available at MI-Partners. A global outline of the set-up is shown in Figure 3, where the shield is depicted as 'Thermal system'.

Numerical analysis on thermal responses

A transient thermal model based on the design of the shield was built in ANSYS Workbench. The model is used for calculating expected thermal responses of the shield resulting from fluctuating cooling water temperatures. The geometry is directly imported from 3D CAD models. A top view with the sensor positions is shown in Figure 2.

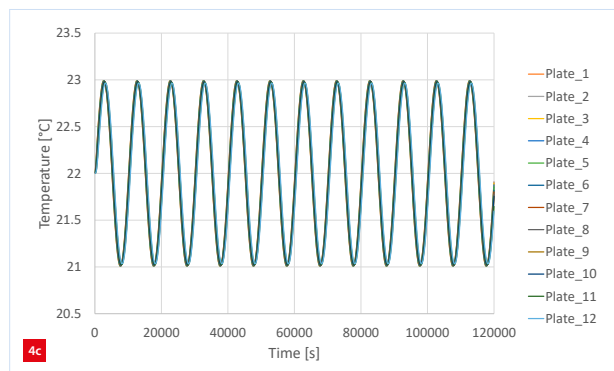
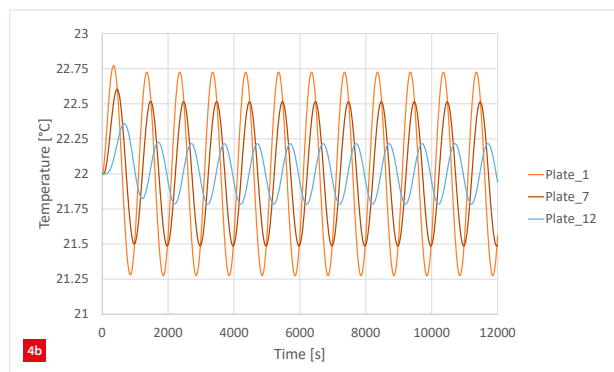
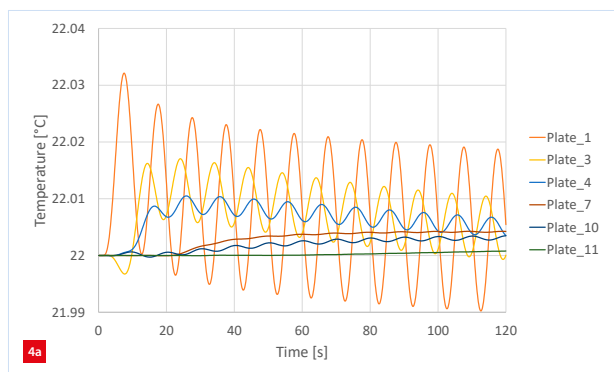
Relevant material properties have been taken from supplier data and/or standard textbook references. The glue is not modelled as a physical material volume since its very small thickness would result in undesired mesh refinement. Therefore, the glue layer is modelled as a contact with a specific heat transfer coefficient between the glued objects (tube and plate). The heat transfer coefficient value is determined from the thermal conduction coefficient of the glue and the glue layer thickness, resulting in $h_{c, \text{glue}} \sim 1,800 \text{ W} \cdot \text{m}^{-2} \cdot \text{K}^{-1}$. Water cooling in the channel is modelled by thermal flow elements. The water flow is set to 1 l/min, and the heat transfer coefficient between water and channel wall is based on this flow and the pipe inner diameter [1], resulting in $h_c \sim 2,838 \text{ W} \cdot \text{m}^{-2} \cdot \text{K}^{-1}$.

Global temperature fields in shield, channel and water have been determined as results of the model calculation. Next to

that, temperature responses at sensor locations have been determined from analysis results, enabling comparison between model calculations and experiments.

Analysis results

In the thermal model, the cooling water supply temperature is prescribed by a sinusoidal function in time with a frequency f and an amplitude ΔT . Expected responses at the sensor positions on the shield are determined using the thermal model. Temperature responses will have the same frequency f as the induced fluctuation on the cooling water. The amplitude of the temperature response on a certain location is dependent on thermal behaviour of the part of the shield between the sensor position and the cooling water. A higher thermal resistance, for instance, will result in a lower amplitude of the thermal response.



Resulting temperature responses at sensor locations for three frequencies.
(a) 0.1 Hz.
(b) 0.001 Hz.
(c) 0.0001 Hz.

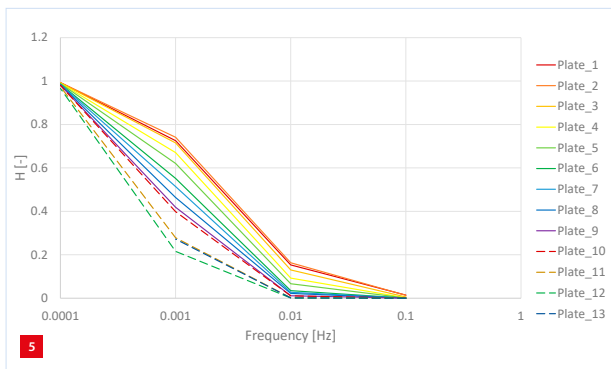
The ratio between amplitudes of a thermal response at a sensor position and the fluctuation of the water is the so-called magnitude (H) of the frequency response function (FRF), which is a representative measure for thermal behaviour. FRF magnitudes are also dependent on the frequency of fluctuation of the cooling water. Therefore, FRF magnitudes were determined by performing model calculations for different frequencies. The amplitude of the input (i.e. the prescribed cooling water temperature) in analyses was chosen to be 1 °C.

Figure 4 shows some examples of resulting temperature responses at the sensor locations for different frequencies. For the lowest frequency (Figure 4c), all temperatures on the shield follow the fluctuating water temperature, having almost the same amplitude as the water (1 °C). For higher frequencies, the response amplitudes drop. Because of thermal resistance and thermal mass of the structure between the sensor locations and the water, temperature fluctuations at sensor locations cannot follow the fluctuation of the water completely, resulting in reduced amplitudes. This effect is stronger for increasing frequencies. This shows that measuring at different frequencies is suitable for characterising thermal behaviour. Furthermore, differences in resulting amplitudes occur between individual sensors, resulting from their respective thermal coupling to the water.

Figure 5 shows FRF magnitudes for the sensor locations on the shield at different frequencies resulting from numerical analysis. As expected, for a frequency of 0.0001 Hz the FRF magnitudes approach 1 (plate temperature fully follows water temperature fluctuation), whereas for a frequency of 0.1 Hz the FRF magnitudes approach zero (shield will not follow water temperature fluctuations due to thermal mass and thermal resistances). For the shield, frequencies of 0.0001 Hz and lower are expected to have FRF magnitude 1, and frequencies of 0.1 Hz and higher are expected to have FRF magnitudes of approximately zero. In between these frequencies, FRF magnitudes of different values between 0 and 1 are expected for the individual sensor locations. Therefore, 0.001 Hz and 0.01 Hz are the frequency levels of interest for performing measurements and thermal qualification.

Decreased thermal contact of the glue layer

Using the thermal model, the effect of reduced thermal contact between channel and plate resulting from the glue layer is investigated. The value of the heat transfer coefficient between channel and plate has been reduced from 1,800 to 900 W·m⁻²·K⁻¹, and resulting FRF magnitudes have been determined. Resulting FRF magnitudes of all sensors for the frequencies of interest (0.01 Hz and 0.001 Hz) are plotted in Figure 6. The figure shows FRF magnitudes as a bar graph.



Calculated FRF magnitudes, representing the amplitude ratios of sensor fluctuation and supply water fluctuation, at sensor locations for several frequencies of the fluctuating water temperature.

The height of the bar corresponds to the FRF magnitude of the respective sensor. Blue and green bars correspond to thermal contact values of $1,800 \text{ W}\cdot\text{m}^{-2}\cdot\text{K}^{-1}$ (expected thermal contact) and $900 \text{ W}\cdot\text{m}^{-2}\cdot\text{K}^{-1}$ (assumed reduced thermal contact), respectively.

Looking at absolute values, it is concluded that FRF magnitudes are higher for lower frequencies. This can be explained as an effect of the shield's thermal mass. Furthermore, FRF magnitudes corresponding to higher sensor IDs are lower than FRF magnitudes corresponding to lower sensor IDs. This can be explained by the fact that low sensor IDs correspond to locations near the supply of the cooling water, while higher sensor IDs correspond to more downstream locations and plate corners. Sensor positions near the water supply have a stronger thermal coupling to the water entrance temperature than sensor positions further downstream or on positions further away from the channel (plate corners).

Comparing the blue and green bars shows that for a frequency of 0.001 Hz (Figure 6a) all green bars are lower than corresponding blue bars. This means that for each sensor, reduced thermal contact of the glue layer leads to a reduced thermal coupling between the water supply

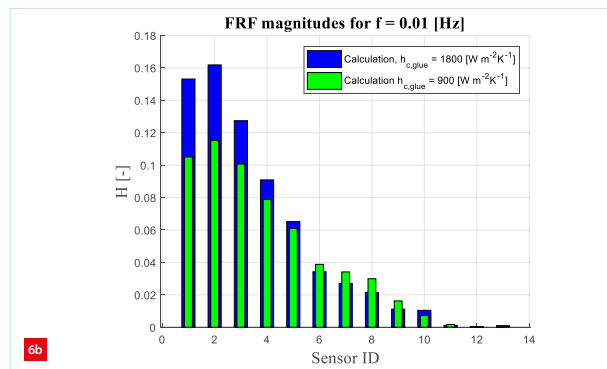
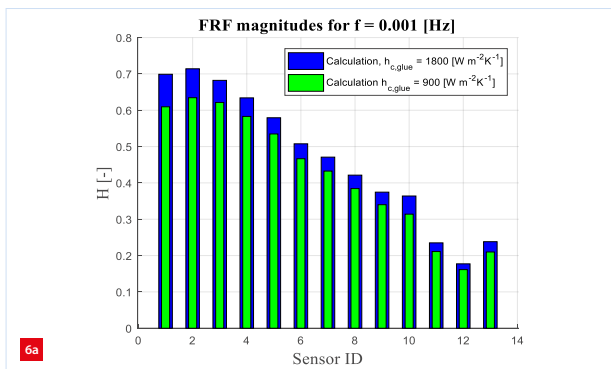
temperature and the sensor location. This is as expected since a reduced thermal contact leads to reduced heat transfer between water and plate.

However, for the frequency of 0.01 Hz (Figure 6b), green bars corresponding to sensor IDs 1 to 5 are lower than corresponding blue bars, while green bars corresponding to more downstream sensor locations (sensor IDs 6 to 9) are higher than corresponding blue bars. This seems remarkable at first sight because it would mean that reducing the thermal contact of the glue layer would lead to increased thermal coupling between supply water and downstream locations.

However, this can be explained because the overall plate temperature does not follow the fluctuation of 0.01 Hz very well. FRF magnitude values obtained for 0.01 Hz are far lower than 1, meaning that the fluctuation in plate temperature is far lower than the fluctuation of the water temperature. Therefore, the plate will mainly act as a thermal mass, absorbing heat from the water without fluctuating too much in overall temperature itself. Heat absorption by the plate from the water will result in nearby sensor fluctuation, but also in reduced temperature fluctuation of the water. Therefore, temperature fluctuation of the water will gradually decrease along the channel, also resulting in reduced fluctuation at downstream sensors.

This effect is weaker for reduced thermal contact between the water and the plate. If the thermal coupling between the water and the plate is worse, heat absorption by the plate will be less, and the temperature fluctuation of the water will remain further downstream. Reduced thermal contact will therefore lead to reduced FRF magnitudes for sensors near the supply water but to increased FRF magnitudes for downstream sensors.

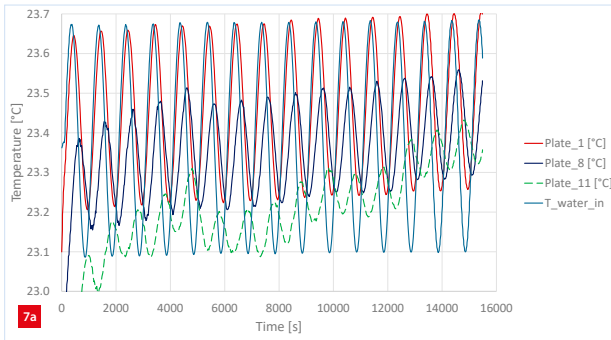
Generally speaking, one can conclude that a better thermal contact of the glue layer will result in higher FRF magnitudes for initial sections of the channel for



FRF magnitudes of all sensors for two frequencies, based on analysis data with glue layer thermal contact values $1,800 \text{ W}\cdot\text{m}^{-2}\cdot\text{K}^{-1}$ (base assumption) and $900 \text{ W}\cdot\text{m}^{-2}\cdot\text{K}^{-1}$ (reduced value).

(a) 0.001 Hz .

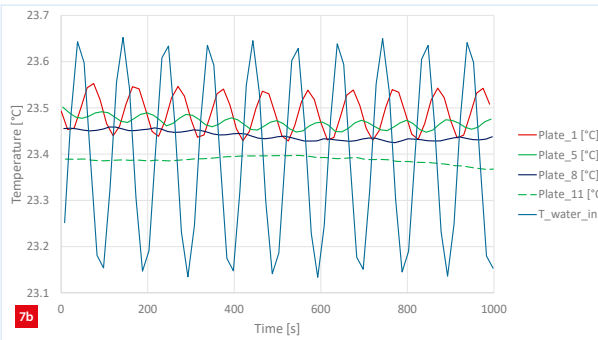
(b) 0.01 Hz .



Resulting temperature responses at the sensor locations for two frequencies.

(a) 0.001 Hz.

(b) 0.01 Hz.



both frequencies. For a frequency value of 0.001 Hz, FRF magnitudes will also be higher for downstream sensors and sensors at the corner locations of the plate, whereas for a frequency value of 0.01 Hz the FRF magnitudes of downstream and corner sensors will be lower.

Measurement results and qualification

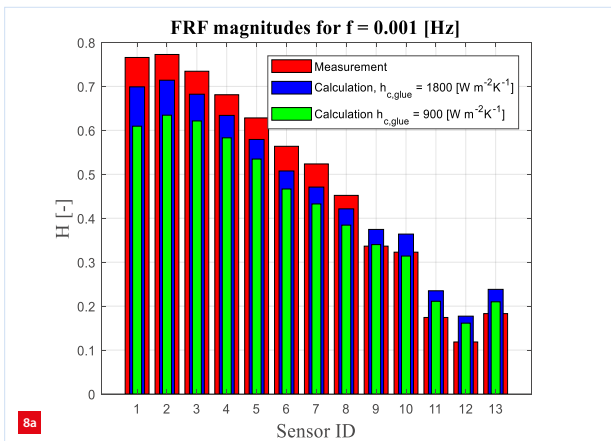
Measurements with a sinusoidal fluctuation of the water temperature were performed at frequencies of 0.001 Hz and 0.01 Hz. Measured temperature responses are shown in Figure 7. Periodic signals with the same frequency as induced on the supply water were indeed found. For the frequency of 0.01 Hz, the responses are not so smooth since the number of data points per fluctuation period is limited because of the 15-s time-step of the data-logger (time required to scan all sensors). For the lower frequency (0.001 Hz) smoothness of the graph is far better since the period of fluctuation is 10 times larger, while the time-step of the data-logger remained the same.

The sampling frequency of the data-logger is 1/15 Hz. Based on the Nyquist criterion, fluctuating signals with frequencies below 1/30 Hz can be reconstructed from measured data. As both frequencies of interest used in the measurements are below this value, fluctuating signals

can be accurately reconstructed from measured data. This was achieved by extracting periodic functions of given frequencies of interest from the measured data using Fast Fourier Transform theory.

As a result, periodic functions for both frequencies were found, and corresponding FRF magnitudes were determined. The values found from measured data together with the values found from analysis results are presented in Figure 8. This figure is nearly identical to Figure 6. The only difference is addition of the red bars, representing FRF magnitudes obtained from measurement data.

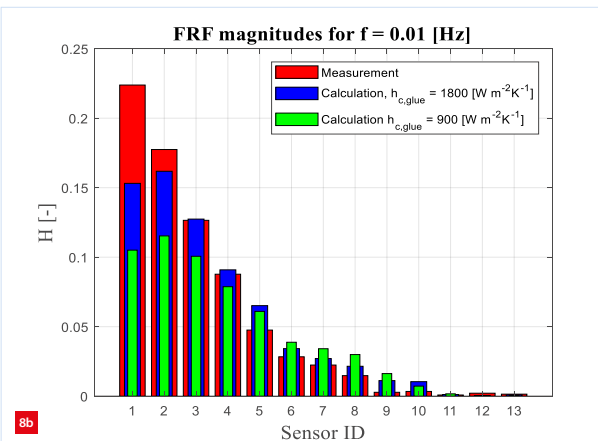
As can be seen in the figure, the global profile of the bars shows good agreement between measurements and calculations for both frequency values. For low sensor IDs (sensors near the water supply), FRF magnitudes based on measurements are higher than FRF magnitudes based on analysis results. For a frequency of 0.01 Hz, the height of the red bars drops below the height of blue and green bars for downstream sensor positions. This is expected behaviour as was described previously. Based on this, one could conclude that the thermal connection between the channel and the plate in the measurement is better than the expected value in calculations.



FRF magnitudes of all sensors for two frequencies.

(a) 0.001 Hz.

(b) 0.01 Hz.



For a frequency of 0.001 Hz, the red bars remain higher than blue and green bars for more downstream sensors as could also be expected from the previous explanation, although that doesn't hold for sensor IDs 9 to 13. Reduced FRF magnitudes of sensors 9 to 13 at a frequency of 0.001 Hz may be explained by environmental disturbances. Sensors 9 to 13 are all sensors near the edge of the shield. Since these sensors are further away from the cooling channel, their responses are also less strongly influenced by the thermal contact between channel and shield and will be affected more by other effects like environmental disturbance or overall shield thermal mass.

Based on these results, it is concluded that the thermal performance of the shield is globally as expected from the design, or even slightly better. It is concluded that the shield will also meet thermal specifications under operation since that was also expected from similar analysis during the design phase. Based on this, the shield is accepted for its thermal application.

Conclusion and recommendation

Frequency-based thermal qualification is a powerful tool for analysing thermal system performance. It can be used for approval of thermal systems, without very stringent demands on environmental conditions. At MI-Partners all necessary equipment and relevant expertise are available for performing thermal qualification.

In the study as presented here, thermal qualification on a single product is performed by comparing measured behaviour to expected behaviour from simulation. By derivation of a simple pass/fail criterion instead of comparing graphs for each product, the method of thermal qualification could possibly be useful for application in a volume production environment.

REFERENCE

[1] F.P. Incropera and D.P. DeWitt, *Fundamentals of Heat and Mass Transfer*, 5th Ed., Wiley, 2002.

LESS
Vibrations

BETTER
Results



Solutions and products against vibrations:

- FAEBI® rubber air springs
- BiAir® membrane air springs
- Mechanical-pneumatic level control systems
- Electronic Pneumatic Position Control EPPC™
- Active Isolation System AIS™
- Customized laboratory tables
- and more...



Your Bilz contact in the Netherlands:



OUDE REIMER

Willem Barentszweg 216 • NL-1212 BR Hilversum • phone: +31 35 6 46 08 20 • info@oudereimer.nl • www.oudereimer.nl

ENCODERS GRADUATING TO EXTREME PRECISION

A revolutionary development in optical displacement metrology has been the transition from free-space laser interferometers to extreme-precision optical encoders for positioning measurements in semiconductor photolithography systems. An increasingly demanding error budget for stage motion control has mandated a dramatic reduction in sensitivity to air turbulence and refractive index changes that is only achievable with multi-dimensional sensors with intrinsically short air paths. Here we describe the design, implementation and performance of these new optical heterodyne encoder systems, which achieve sub-nm displacement measurements for stages moving at over 8 m/s.

VIVEK BADAMI, JAN LIESENER AND PETER DE GROOT

The challenge

The history of the fabrication of semiconductor devices is characterised by astonishing breakthroughs in the number of transistors in a single data processor, now approaching 20 billion. The fabrication of circuits and memory at these densities relies on as many as 100 overlaying patterns created by high-speed lithographic exposure of photoresist, followed by chemical processing and reinsertion into a photolithography system for the next layer.

Each new pattern on a wafer in production is registered with the previous layers to a fraction of the 10-nm minimum critical dimension (CD) of individual transistors. The stage position measurement is only one part of the uncertainty budget, leading to demanding, sub-nm uncertainty allocation to stage metrology [1]. Wafer throughput requirements of 15 s per cycle on each wafer drive stage speeds to greater than 1 m/s, with displacements in the order of 0.5 m [2].

Until recently, stage metrology subsystems for semiconductor lithography consisted almost entirely of line-of-sight laser interferometers. These systems are highly-evolved versions of Michelson two-beam interferometers designed to monitor displacements and changes in stage orientation using heterodyne detection [3]. As CD values have decreased, the use of interferometers with long path lengths has reached a practical limit: fluctuations or turbulence in the air and environmental sensitivities related to variations in air index have proved to be the largest contributors to stage metrology error. For extreme ultraviolet (EUV) systems working in a vacuum, this error source is less of an issue; but the majority of semiconductor exposure processes still take place in air and the resulting air turbulence from airflow, stage motions and other disturbances contributes as much as 80% of the error budget for the stage metrology [4].

In anticipation of the air-turbulence limit, serious attempts have been made to compensate for the refractive index of air using dispersion interferometry [3, 5, 6]; but these efforts have been overtaken by ever-tightening requirements. Another solution is needed.

The solution

The solution to the limitations imposed by air turbulence and environmental effects relies on the scaling of the magnitude of these sensitivities with the length of the air paths traversed by the interferometer beams. Shorter air paths result in a smaller contribution from these disturbances. Optical encoder systems replace the mirror with a diffraction grating (a substrate with periodic structures). Encoders shorten the air path from hundreds of mm in length typical of conventional interferometers to a constant length of just a few mm, significantly reducing air turbulence as an error source. Figure 1a and 1b contrast these two arrangements.

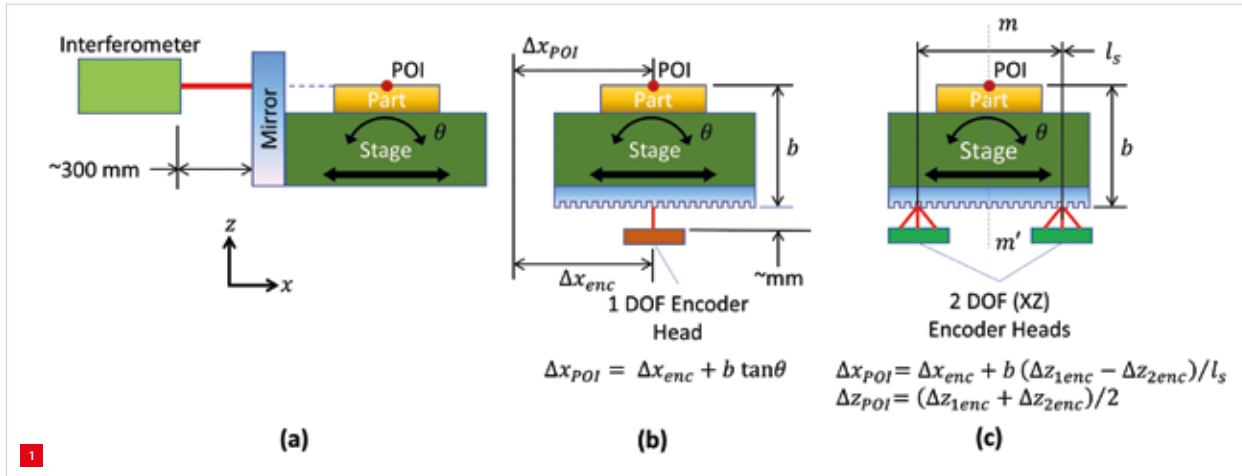
A long-standing limitation of encoders has been the inability to locate encoders in multi-degree-of-freedom (multi-DoF) stage systems in compliance with the Abbe principle, which requires that the line of measurement pass through the point of interest (POI) [7, 8]. Line-of-sight interferometers easily achieve this (Figure 1a), while a single 1-DoF encoder in a multi-DoF application must account for the Abbe offset b and the stage rotation θ (Figure 1b).

As shown in the example in Figure 1c, multi-DoF encoders address this by providing displacement information in both the x and z direction that enables the measurement of the angular error motions of the stage for the compensation for the effects of the Abbe offset in the x direction as well as

AUTHORS' NOTE

Dr. Vivek Badami is a technology fellow in the Innovations Group at Zygo Corporation, headquartered in Middlefield, CT, USA. Dr. Jan Liesener is a senior scientist and inventor in the field of interferometry. Dr. Peter de Groot is the executive director of R&D at Zygo Corporation.

ernesto.abruna@ametek.com (enquiries)
www.zygo.com



Comparison of interferometer and encoder arrangements. Figures not to scale.

(a) Interferometer in compliance with the Abbe principle, but with a large air path length.

(b) 1-DoF encoder with ~mm scale air path, but in violation of the Abbe principle.

(c) Multiple 2-DoF encoders enabling compensation of Abbe errors while preserving a low sensitivity to air turbulence and environmental effects.

providing an effective line of measurement through the POI in the z direction. Using several multi-DoF encoders in conjunction with two-dimensional (2D) gratings enables extension of this principle to effectively eliminate Abbe errors in all measurement axes that result from rigid-body motions.

Encoders based on heterodyne interferometry

Encoders face another challenge in the intrinsically low light efficiency from a grating target. The net efficiency for a double-pass encoder with a 2D grating can be as low as 1%. It is a further system requirement that multiple encoders share the same light source, preferably at the familiar 633-nm Helium-Neon (HeNe) laser wavelength. The solution to this challenge is a proprietary light source combined with heterodyne signal detection – a combination that has fundamental advantages in achieving the high signal-to-noise ratio (S/N) that is essential for sub-nm performance at high speed [9].

Heterodyne detection

Our heterodyne encoder systems use a proprietary 20-mW, frequency-stabilised, single-mode HeNe laser [10]. The output beam is split into two collinear, orthogonally polarised beams that have a fixed optical frequency difference (the split frequency) between them by means of an acousto-optical modulator. Within the encoder, these two polarised beams play the role of measurement and reference beams of an interferometer, with the grating being an integral part of the measurement path.

The beams interfere after passing through a mixing polariser at the output. The frequency split between the two beams creates a continuous sinusoidal beat signal, even with a stationary target. As the target moves, this changes the optical path length, and the receiver electronics detect

a time-varying phase change at the split frequency that is proportional to the displacement.

Heterodyne detection provides important advantages over homodyne detection, the chief being a significantly improved S/N thanks to the shift in the operating point of the interferometer away from the high $1/f$ noise background in the low-frequency region of the spectrum. A further reduction in noise follows from using fewer detectors per measurement channel when compared to homodyne interferometers.

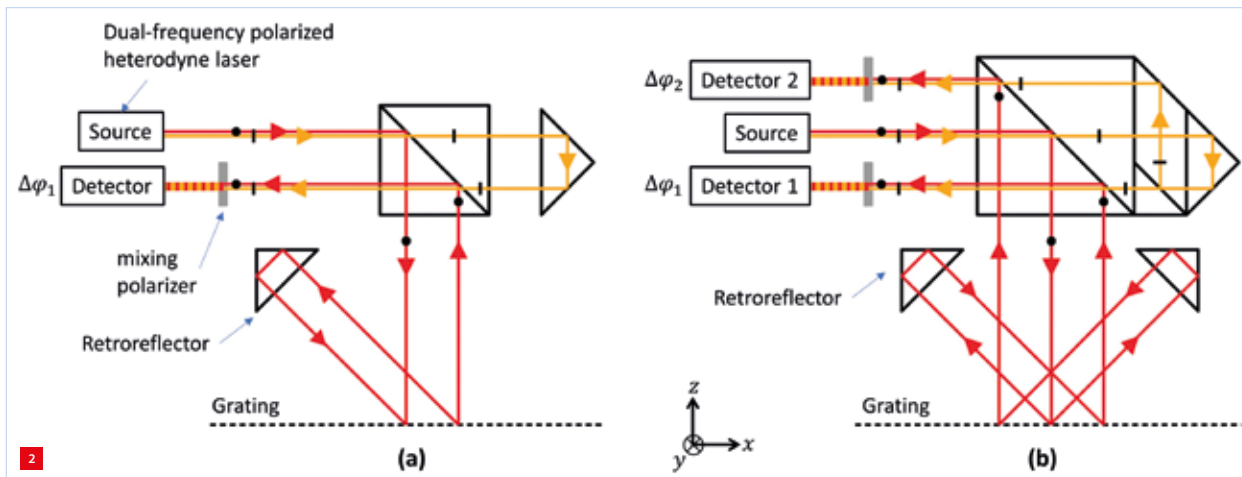
Encoder design

A fundamental challenge of encoder designs is to achieve high-resolution measurements of in-plane and out-of-plane motions while accommodating tip and tilt of the grating. Figure 2a shows one of our interferometric encoder designs where a retroreflector reverses the measurement beam's path after its encounter with the grating [11]. The reversal via a retroreflector makes the final beam angle independent of grating rotation about x , y and z , thereby maintaining adequate signal strength over realistic rotations. The double-pass beam geometry doubles the sensitivity to grating motion, at the expense of radiometric efficiency.

The basic configuration of Figure 2a is sensitive to displacements both in the in-plane x and out-of-plane z directions, i.e. the measured phase change $\Delta\phi_1$ is a linear combination of the two displacements. A second measurement channel as shown in Figure 2b provides an additional phase change $\Delta\phi_2$ that allows the electronics to separate these two motions. Solving for displacements Δx and Δz from the two measured phase changes $\Delta\phi_1$ and $\Delta\phi_2$ results in:

$$\Delta x = c_x (\Delta\phi_1 - \Delta\phi_2)$$

$$\Delta z = c_z (\Delta\phi_1 + \Delta\phi_2)$$



Encoder head designs.

Input and output beams are fibre-delivered from a remote source and to remote detectors rendering the head totally passive.

(a) A single detector providing information about the grating's motion in x, while also being affected by motion in z.

(b) Two measurement channels distinguishing between the grating's x and z motions.

Here, c_x is derived from the grating pitch and c_z is derived from the wavelength and the grating pitch. Combining multiple encoders oriented in different directions and viewing different areas of a 2D grating provides full 6-DoF sensing with Abbe offset compensation.

Advanced configurations

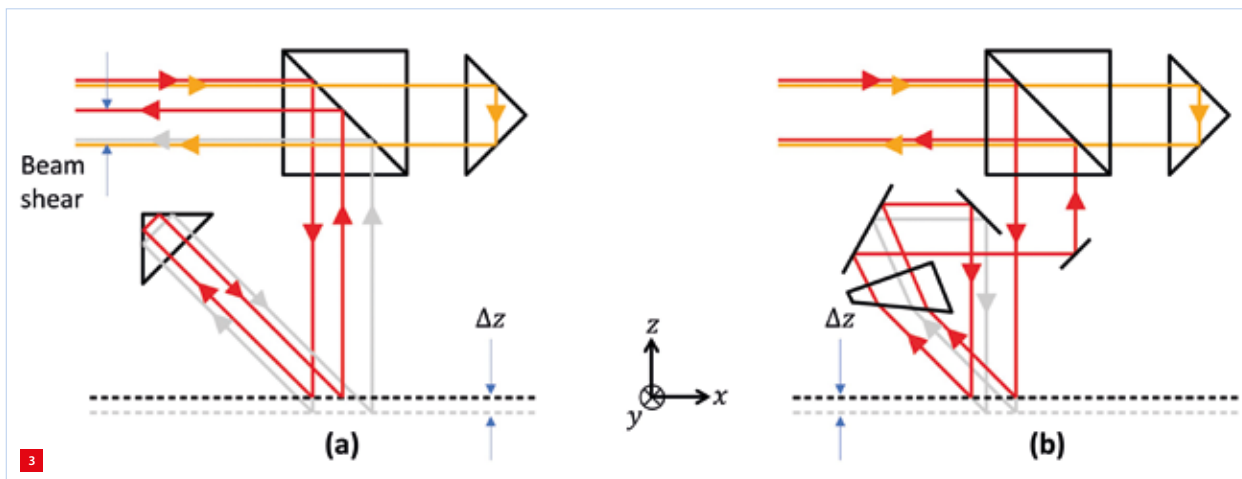
Although stages in lithography applications nominally move within the xy plane, encoders also monitor out-of-plane z motions over a range that can sometimes reach 1 mm as the stage tips, tilts and translates to accommodate variations in wafer flatness and focus position.

Figure 3 demonstrates how the grating's motion in z creates a beam shear between the orange reference and the red measurement beam in the basic encoder design of Figure 3a. Excessive beam shear of the order of the beam radius or larger reduces the signal significantly.

Depending on the encoder location in the photolithography system, accommodation of the required stage motions may warrant more advanced optical designs.

Choosing a larger beam to increase the z range would be an obvious solution; but the need for compact designs usually rules out this otherwise straightforward option. Figure 3b shows a superior beam geometry for extending the z range, which – during the second diffraction – fully compensates the shear created during the first diffraction. As long as the internally sheared beam clears limiting apertures, this advanced design maintains full signal strength over a wide range of z positions [12].

For encoders to provide accurate measurements, the effects of unintended beam paths through the optical system need to be minimised. So-called ghost beams that pollute the



Beam shear created by grating motion in z. The gray beams are those corresponding to the grating in its nominal position before displacement in z. In each case only one diffracted order is shown for simplicity.

(a) Large beam shear in the basic encoder design.

(b) No beam shear in a more advanced design

Table 1
Summary of key specifications for ZYGO heterodyne encoders.

Range in x and y direction	Determined by length of grating
Range in z direction	± 1 mm
Max. velocity (with 1 μm grating pitch)	8.1 m/s
Typical grating tilt range	± 10 mrad
Cyclic error	< 50 pm
Digital resolution	7.6 pm
Data rate	10 MHz
Operating wavelength	633 nm
Data interface	sRIO

encoder's optical signal arise from polarisation leakage or unwanted reflections from various components. While advanced signal processing can reduce the effects (as described below), prevention of ghost beams in the first place is always preferable. A variety of strategies can be applied that separate the ghost beams from the desired beams spatially or angularly, e.g., by means of glass wedges or birefringent prisms [13]. While the exact heterodyne encoder head designs and specifications depend on the particular application, Table 1 provides a general sense for the key performance specifications.

Design for repeatability

Successful registration of features between the various layers of an integrated circuit requires consistent, repeatable stage positioning. Good encoder design therefore places a premium on repeatability, and seeks to minimise noise and drift that would otherwise compromise consistent results in the stage metrology. Here we consider a few of these

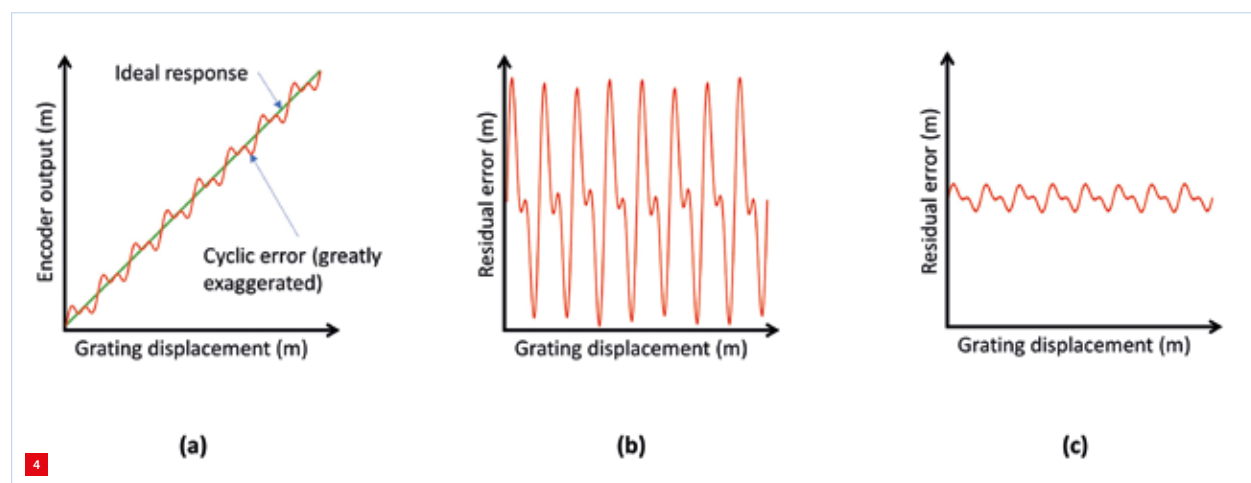
potential error sources and their mitigation.

Heterodyne encoders receive the light from the two-frequency laser source via optical fibres. Temperature- and strain-induced phase changes between the two frequencies as they propagate through the fibres manifest themselves as erroneous displacements. Specialised optics within the encoder head interferometrically measure and compensate these phase changes in real-time.

While the in-plane measurements are independent of the wavelength, any wavelength instabilities affect the measurement repeatability through unequal measurement and reference paths. Specialised high-power, frequency-stabilised HeNe laser sources with stabilities of a few parts per billion (ppb) in combination with the small path imbalances provide sub-nm stabilities over times commensurate with lithographic cycle times [10].

Interestingly, the traceability path to the unit of length for encoder systems is through the grating calibration, rather than directly to the wavelength of light. On balance, this turns out to be an advantage, as reliance on a material artifact (the grating) reduces sensitivity to short-term environmental changes in temperature and pressure thanks to the thermal and mechanical stability of the grating material. This is a distinct advantage in the arena of microlithography, where stability and precision far outweigh the need for accuracy.

A source of non-repeatability common to many interferometers and encoders are cyclic or periodic errors (also referred to as interpolation errors) [14]. These errors have periods that are related to the wavelength or the grating pitch and lead to periodic deviations of the measured displacement from the true displacement as shown in Figure 4.

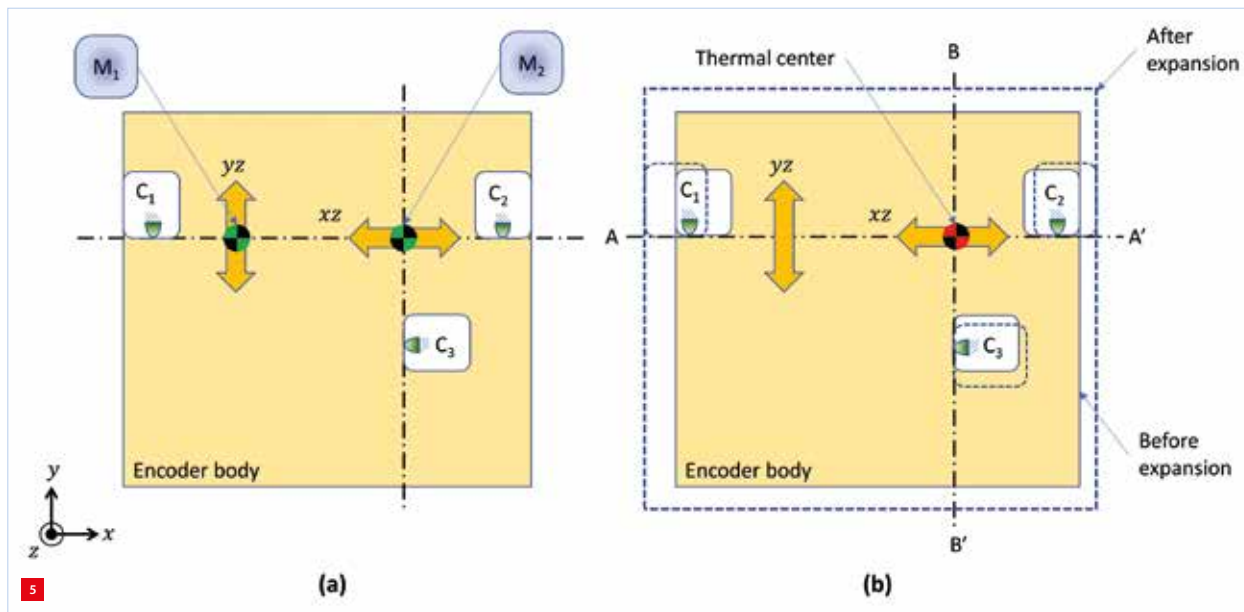


Cyclic or periodic error.

(a) Encoder response with the deviation of the measured displacement from the actual displacement.

(b) Residual error magnitude after optical correction of 0.4 nm.

(c) Residual error after optical and electronic correction reduced to 0.04 nm.



Minimisation of thermal sensitivity by strategic arrangement of constraints C_1 , C_2 and C_3 .

(a) Measurement points M_1 and M_2 measure in the yz and xz directions, respectively.

(b) M_2 is arranged to coincide with the thermal centre while M_1 is located on AA' such that any expansion only results in motions in the non-sensitive direction of M_1 .

The mitigation of these errors includes both optical measures [15] and the detection and removal of residual parasitic signals electronically [16, 17], with the electronic reduction affording an additional order of magnitude reduction over the already sub-nm cyclic error after optical correction as shown in Figure 4c.

The sensitivity of the encoder head to changes of temperature can be an important source of measurement drift. These contributions arise from deformations of the encoder structure, bulk changes in the refractive index of glass components, birefringence from thermal stresses and thermal deformation of the adhesive bonds within the encoder assembly. The largest of these contributors is often the temperature-induced motion of the effective measuring point of the encoder relative to the encoder mount.

A combination of low-CTE materials, careful design of the constraint system to accommodate thermal expansion and strategic location of thermal centres (Figure 5) produce sub-nm contributions in the temperature environments typically found in lithography machines [18]. The choice of adhesives and the design of joints requires careful consideration to accommodate differential expansion between optics with different CTE values while also preventing excessive stresses from developing – stresses which result in birefringence and localised index changes.

Summary

As we have seen, the basic problem posed by photolithographic stage positioning reflects the global

technology and manufacturing trends towards ever more demanding requirements, with a current requirement for controlling the position of a stage moving at up to 8 m/s to sub-nanometer precision. Turbulent airflows and the environmental sensitivity of the air index have made traditional long-path interferometric solutions untenable for the latest generation of wafer fabrication systems in the majority of photolithography systems, leading to the introduction of short-path, 2D grating encoders – an enabling technology that until recently simply was not up to the task.

The heterodyne optical encoder solution is an excellent example of interdisciplinary precision engineering in action. Every aspect of the development of encoders over the last decade has required significant advances, starting with innovative optical designs to accomplish multi-dimensional sensing, to the mechanical design for thermal insensitivity, temporal stability and manufacturability.

The laser-heterodyne system involves new light sources, advanced optical and electronic cyclic error reduction, fibre-optic delivery, and highly complex assemblies of precision-fabricated optical components. Far from being demonstration experiments of the state-of-the-art, these revolutionary designs are purpose-built, practical implementations that must satisfy daunting space, cost and performance constraints on a routine production basis. It perhaps goes without saying that these requirements are not stationary – they will continue to challenge us to precision engineer creative solutions going forward.

REFERENCES

- [1] Schmidt, R.-H.M., "Ultra-precision engineering in lithographic exposure equipment for the semiconductor industry", *Philosophical Transactions of the Royal Society of London A: Mathematical, Physical and Engineering Sciences*, 370(1973), pp. 3950-3972, 2012.
- [2] Butler, H., "Position Control in Lithographic Equipment [Applications of Control]", *IEEE Control Systems*, 31(5), pp. 28-47, 2011.
- [3] Badami, V.G., and de Groot, P.J., "Displacement Measuring Interferometry", in *Handbook of Optical Dimensional Metrology*, K.G. Harding (Ed.), Taylor & Francis, Boca Raton, pp. 157-238, 2013.
- [4] Shibasaki, Y., Kohno, H., and Hamatani, M., "An innovative platform for high-throughput high-accuracy lithography using a single wafer stage", in *Proc. SPIE 7274, Advanced Lithography*, pp. 72741I-1 – 72741I-12, 2009.
- [5] Hill, H.A., and de Groot, P., "Air turbulence compensation for sub-nanometer displacement measuring interferometry", in *Proc. ASPE Spring Topical Meeting on Precision Interferometric Metrology*, Tucson, AZ, Abstract no. 25, 2000.
- [6] Jang, Y.-S., and Kim, S.-W., "Compensation of the refractive index of air in laser interferometer for distance measurement: A review", *International Journal of Precision Engineering and Manufacturing*, 18(12), pp. 1881-1890, 2017.
- [7] Abbe, E., "Messapparate für Physiker", *Zeitschrift für Instrumentenkunde*, 10, pp. 446-448, 1890.
- [8] Kunzmann, H., Pfeifer, T., and Flügge, J., "Scales vs. laser interferometers performance and comparison of two measuring systems", *CIRP Annals-Manufacturing Technology*, 42(2), pp. 753-767, 1993.
- [9] Jacobs, S.F., "Optical heterodyne (coherent) detection", *American Journal of Physics*, 56(3), pp. 235-245, 1988.
- [10] Holmes, M.L., Shull, W.A., and Barkman, M.L., "High-powered, stabilized heterodyne laser source for state-of-the-art multi-axis photolithography stage control", in *Proc. of the 15th euspen International Conference*, Leuven, Belgium, pp. 135-136, 2015.
- [11] Deck, L.L., de Groot, P.J., and Schroeder, M., "Interferometric encoder systems", US Patent No. 8,300,233, 2012.
- [12] de Groot, P., and Liesener, J., "Double pass interferometric encoder system", US Patent No. 9,025,161, 2015.
- [13] de Groot, P.J., and Schroeder, M., "Interferometric heterodyne optical encoder system", US Patent No. 9,140,537, 2015.
- [14] Badami, V.G., and Patterson, S.R., "A frequency domain method for the measurement of nonlinearity in heterodyne interferometry", *Precision Engineering*, 24(1), pp. 41-49, 2000.
- [15] de Groot, P., "Jones matrix analysis of high-precision displacement measuring interferometers", in *Proc. 2nd Topical Meeting on Optoelectronic Distance Measurement and Applications (ODIMAP II)*, pp. 9-14, 1999.
- [16] Hill, H.A., "Systems and methods for characterizing and correcting cyclic errors in distance measuring and dispersion interferometry", US Patent No. 6,137,574, 2000.
- [17] Demarest, F.C., "Cyclic error compensation in interferometric encoder systems", US Patent No. 8,913,226, 2014.
- [18] Badami, V.G., "Thermally stable optical sensor mount", US Patent No. 9,200,892, 2015.

LET'S SHAPE THE FUTURE TOGETHER

LOOKING FOR
ENGINEERS
MECHANICS, AUTOMOTIVE,
MECHATRONICS,
ANALYSIS

WE DEVELOP
**ADVANCED
INTELLIGENT
SYSTEMS**
FOR OUR BUSINESS SECTORS

OUR BUSINESS SECTORS:
**HIGH TECH, AUTOMOTIVE
& INDUSTRIAL VEHICLES,
MACHINERY**

WE ARE ALWAYS LOOKING FOR
**TALENTED
ENGINEERS**
WHO CAN STRENGTHEN OUR TEAM



SEGULA Technologies NL, part of SEGULA Technologies Group which operates in more than 30 countries and has more than 12,000 employees. SEGULA Technologies NL is established in 2010 and develops advanced intelligent systems, in particular for the High Tech, Automotive industry and Machinery in the Benelux.



WWW.SEGULA.NL | INFO.NL@SEGULAGRP.COM | T +31 40 85 17 500

COBOTS: NO FAIRYTALE CHARACTERS

Odense, the Danish birthplace of the famous fairytale writer Hans Christian Andersen, hosted the 11th edition of the Expert Days on Service Robotics at the end of February. The event is an initiative by Schunk, a world market leader in gripping systems and clamping technology, and this edition featured topics such as healthcare robot applications, learning, reconfigurable robots, safety, and cobots, i.e. collaborative robots.

JOS GUNSING

Healthcare

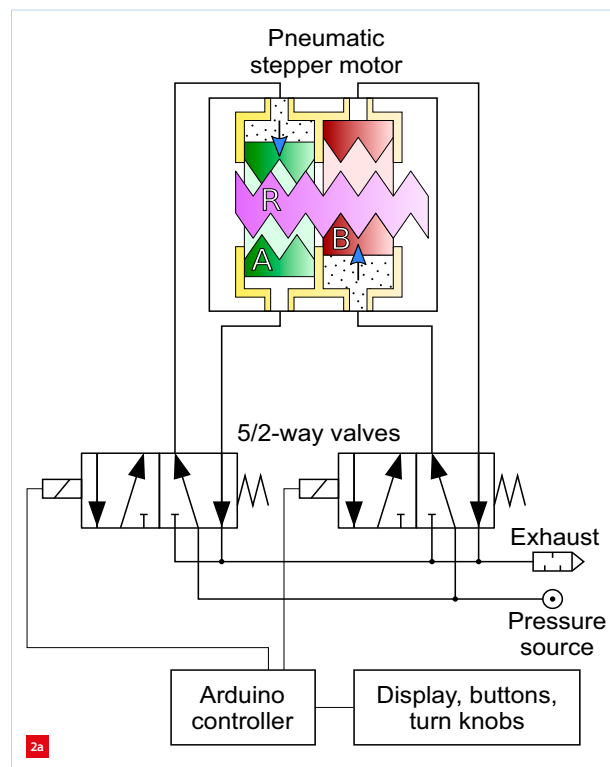
At the 11th Expert Days on Service Robotics [1], the keynote lecture by Stefano Stramigioli, professor of Advanced Robotics in the Robotics and Mechatronics group at the University of Twente (RAM@UT) [2], focused on developments in healthcare robotics. A specific topic he and his group are currently working on is the robotised biopsy-needle-guiding tool for in-MRI application (see Figure 1 and the video [V1]). A major requirement for the equipment involved is MRI-compatibility, i.e. materials being non-magnetic. This has resulted in the development of a pneumatic stepper motor principle (Figure 2 and 3). Over the course of the project the stepping mechanism and its control have been refined further and further, with the latest generation of the guiding tool also containing a long-stroke/short-stroke actuation mechanism for some of the axes.

Wolfgang Ptakek, from the Austrian Center for Medical Innovation and Technology, also gave an interesting lecture on robotically assisted biopsy, but in this case the biopsies are carried out on corpses for medical or forensic tests. Given that within some religions the next of kin do not approve the opening up of a body for such tests, the ability to conduct

a robot-assisted biopsy can help in attaining answers without breaking any prohibitions. The robot and the biopsy tools are guided with the help of a CT scanner. In this environment



Sunram 5, the latest generation of the biopsy-needle-guiding mechanism developed by the Robotics and Mechatronics group at the University of Twente. (Photo courtesy of RAM@UT)



Working principle of a pneumatic stepper motor containing two pistons (A and B) driving a ratchet (R). (Illustrations courtesy of RAM@UT)
(a) Control scheme.
(b) The combination of two pistons successively taking up different states in a cyclic process (state 4 = state 0), to move the ratchet to the right.

AUTHOR'S NOTE

Jos Gunsing is founder/owner of MaromeTech, a technology & innovation support provider, based in Nijmegen (NL).

jos.gunsing@marometech.nl



Physical realisation of the pneumatic stepper motor. (Photo courtesy of RAM@UT)

a more conventional approach, as compared with the above MRI case, can be taken, using a standard robot arm.

Learning

In the area of logistics, two lectures featured the quite different approaches of Amazon and Lidl, respectively. Amazon wants to pick, stow and store goods where variety is almost endless, with hardly any chance that a robot will see a similar product twice during its lifetime, whereas in the case of Lidl, the number of different products is only about 1,700. The main robot task for Lidl is restocking goods in the store, such that the most recently stocked products are placed at the back of the shelf.

In both cases great efforts are being put into product recognition; a lot of products such as bags do not have very well-defined shapes. Here, deep learning and training robots with datasets are the key tasks for covering these issues. Nevertheless, reliable handling/manipulation/gripping of the goods remains a key factor in determining the robustness/reliability of picking, stowing and storing goods.

With respect to learning and programming, both Jan Peters, University of Darmstadt, Germany, and Martin Naumann, drag and bot GmbH, gave an overview of current developments. Peters focuses on efficient imitation learning, where the robot starts with a basic skill set plus learning capabilities, then gradually working towards more complex tasks. Drag and bot, however, is a commercial company building a universal human interfacing 'skin' around several cobot (collaborative robot) systems, such that operators can apply the same way of working/graphical user interface to learning/programming for different cobot types.

Reconfigurable robots

Jamie Paik, professor and director of the Reconfigurable Robotics Lab at École Polytechnique Fédérale de Lausanne (EPFL), Switzerland, gave an inspiring overview of her work; see the video [V2]. With respect to cobots, she speaks about intrinsic softness through material properties



The 'Origami' concept of reconfigurable robots. (Photo by Christoph Belke, courtesy of Reconfigurable Robotics Lab, EPFL)

(e.g. an elastic/elastoplastic skin) or extrinsic softness through elastic elements and/or control technology.

She also discussed the application of pneumatics or vacuum as a soft actuator/gripper technology. It was thought-provoking to see the interest in pneumatics for actuation and gripping in Paik's and Stramigioli's lectures, although choices were made based on very different requirements/boundary conditions. Paik showed an example of an underactuated 'robogami' gripper in which compliancy adaptation facilitates the change from an 'egg' grasp to a precision 'coin' grasp.

Extremely interesting was Paik's lecture on 'Origami' robots (Figure 4), in which rigid parts have been combined with flexible hinges. As an example, the reconfigurable 'Tribot' robot is shown in Figure 5. Here, the hinges are flex PCBs providing electronic control and data communication and power distribution between the joints. The shape-memory-alloy actuator springs are triggered by heat. As the robots are very light, the Tribot can jump seven times its own height.



The reconfigurable Tribot; see text for further explanation. (Photo by Alain Herzog, courtesy of Reconfigurable Robotics Lab, EPFL)



Airskin for operator safety (here only in the gripper area of the robot). (Photo by Jos Günsing)

Safety

A robot/cobot conference cannot be without safety as a standard topic. It is clear that although the ISO safety standards ISO 12100 (safety risk analysis), ISO 10218 (robots & robotic devices) and ISO 15066 (collaborative robots) are available, the translation towards a safe and effective cobot system for a specific application is still a struggle. Developing ways to perform risk assessments in a workable and intuitive way is akin to finding the Holy Grail, and many researchers and engineers in the industry are working on this.

With conventional robots, extra safety can be added by way of an Airskin, a safety skin as an add-on. The principle is based on bumper-like shields/pads that contain enclosed air. The slight air pressure variation when hitting someone or something can be detected with a 9-ms reaction time, upon which the robot can be stopped. The additional cost for a small-sized robot is approximately 8,000-10,000 euro if it is covered with this Airskin completely (Figure 6).

Odense

The choice of Odense, one of the world's hot spots for cobot



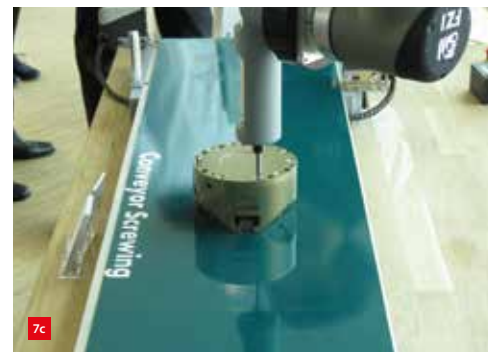
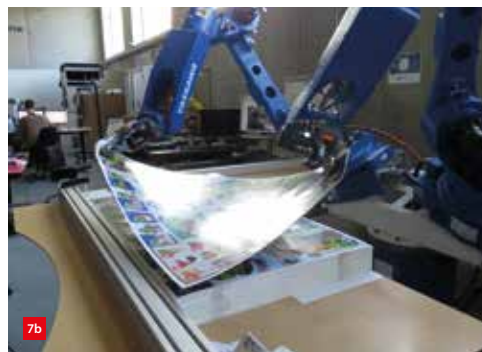
During a visit by the Expert Days participants to the DTI Robot Technology Division, this robot from Universal Robots' first pre-series was spotted in the reception hall. (Photo by Jos Günsing)

research and industry, as the host city for the Expert Days was a logical one. To start with, the Dansk Teknologisk Institut (DTI) [4] with its Robot Technology Division is located here; it can be compared to institutes like the Dutch TNO or the German Fraunhofer-Gesellschaft and works together with universities and companies in applied research. DTI investigates a variety of cobot applications (Figure 7), including logistics, assembly, and aerial and subsea drone inspection.

Universal Robots

In addition, the Odense area is crowded with robotics and automation companies. Some 130 companies on the island of Funen, of which Odense is the capital, are active in this field and over 3,600 people are employed by them, not including those from the strong supplier base in this region.

Odense-based Universal Robots (UR) [5], founded in 2005, is a worldwide leading manufacturer of robust and industrially fit cobots, still with close links to DTI (Figure 8). At UR, several lines of the standardised components for its three robot versions are being



Cobot applications at DTI. (Photos by Jos Günsing)
(a) Picking and manipulating trays or six packs.
(b) Collaboration for sheet picking.
(c) Assembly of products.

assembled with partial automation using the help of, unsurprisingly, UR robots. The production capacity amounts to 80 robots per working day; one year ago UR celebrated its 25,000th delivery.

The UR test room made quite an impression during a visit by the Expert Days participants (Figure 9). Here, the robots are tested and calibrated, and perform a short 'burn-in' test run. The company presentation was focused on UR+: UR co-operates with companies such as Schunk and Cognex in order to complement its robot capabilities with their gripping and vision technologies, respectively, and thus deliver easy-to-teach complete cobot functionality.

Conclusion

Looking back over the past few years, it is clear that the cobot has already left the research arena. The focus of the presentations during the 11th edition of the Expert Days had moved towards artificial intelligence, although it was emphasised by many speakers that more refined gripping and dexterity, the combination of accuracy and compliance plus mobility, are still needed, requiring a lot of precision engineering research. Integrating usability, user friendliness and safety, and achieving an acceptable performance/price ratio, are only at the beginning. So a lot of fairytales have still yet to come true.

REFERENCES

- [1] www.expertdays.schunk.com
- [2] www.ram.ewi.utwente.nl
- [3] rr.epfl.ch
- [4] www.dti.dk/specialists/robot-technology-and-automation/39709
- [5] www.universal-robots.com

VIDEO

- [V1] Sunram 5: An MR Safe Robotic System for Breast Biopsy, www.youtube.com/watch?v=QB_iSPMzztY



- [V2] Meet the Paik Lab, www.youtube.com/watch?v=RUWUWW8qZcg



Test room at Universal Robots. (Photo courtesy of UR)

Growing market demand for cobots

To continue to meet the exponentially growing market demand for cobots in the Benelux region, Universal Robots (UR) is intensifying its co-operation with robot integrator Gibas Automation, UR's representative in Benelux since 2010. To this end, the partners will split integration and distribution. From 1 May, the newly established Industrial Cobotics, based in Haaltert, Belgium, will be responsible for distribution and marketing, while Gibas Automation, with headquarters in Nijkerk (NL), will focus entirely on integration and service activities.

WWW.GIBAS.NL
INDUSTRIALCOBOTICS.BE

Making eye surgery more precise

Eye surgeries are always a big challenge, and steady hands are a key requirement.

**Turning ideas
into solutions
with [maxon.com/](https://www.maxon.com/)
Preceyes**

The Dutch company Preceyes developed the world's first robotic system for eye surgery. While the operating surgeon is looking through a microscope, he is operating a joystick whose motion is transmitted to a robotic arm. The robot scales the motion down. This means that when the surgeon moves the joystick by a centimeter, the tip of the robotic arm moves only a millimeter. Meanwhile the other hand performs manual tasks as required. The motions of the robotic arms are performed by the high-precision drive systems of maxon motor.

BOTH ADDITIVE AND SUBTRACTIVE SHAPING WITHOUT RECLAMPING

Okuma is a well-known Japanese provider of highly accurate multitasking machining centres, being able to turn, mill and grind as well. Okuma has recently added Trumpf solid-state lasers to this equipment to enable additive manufacturing with the LMD process: laser metal deposition. A subtractively machined workpiece can thus be given a wear-resistant layer or be submitted to heat treatment in one single clamping operation. The other way round, a 3D-printed object can be accurately finished by grinding.

FRANS ZUURVEEN

Up until recently, 3D printing (also called additive manufacturing, AM) used to be a quite separate manufacturing process, performed on different machines, often at quite different production centres. Okuma, specialised in the delivery of subtractively functioning CNC machines, see Figure 1, became aware of this both virtual and real distance to additively functioning machines. Integrating both shaping methods in one multitasking machine would yield a considerable reduction in time and costs.

That is why Okuma in Japan, represented in the Benelux by Gelderblom, contacted laser application specialist Trumpf in Germany. This resulted in an exclusive partnership, because Okuma did not want to reinvent the wheel of the additive technology, developed by Trumpf as the LMD process. The introduction of a powerful four-kilowatt Trumpf disc laser in the Okuma Laser EX machining centres also had an extra advantage: heat treatments, such as hardening and protective coating of a workpiece, on the spot in the machine.

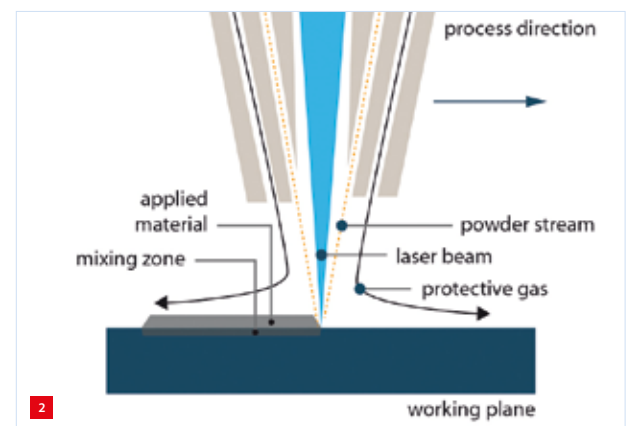
This made Okuma one of the first manufacturers to develop multitasking machines, uniting additive and subtractive manufacturing in one machine. Traditionally all relevant parts of Okuma products, including the Laser EX series, are manufactured by Okuma in its own factories, with the exception of the Trumpf laser gun and various slide roller guides. These Okuma in-house products include drives, motors, encoders, spindles and CNC controls. The machining centre base frame is accurately machined from a rough cast-iron workpiece. Spindles are equipped with roller or ball bearings, resulting in rotational accuracies better than 3 µm.

Laser Metal Deposition

The LMD process is rather easy to understand, see Figure 2. The high-power laser with an adjustable spot diameter between 0.3 and 8.5 mm creates a weld pool on the component surface, see Figure 3, in which a stream of metal powder is automatically added via a nozzle. This results in beads that are welded together to form a line of deposited material.



Subtractive grinding on an Okuma machining centre.



Schematic explanation of the laser metal deposition process. (Illustration: Trumpf)

AUTHOR'S NOTE

Frans Zuurveen, former editor of Philips Technical Review, is a freelance writer who lives in Vlissingen (NL).



The LMD tool, developed by Trumpf, in action on a Laser EX machining centre.

The Trumpf LMD tool applies three streams of metal powder. This makes it possible to create layers of special metal alloys on the workpiece surface by mixing different material powders beforehand. They include powders of iron, nickel, cobalt, aluminium and even carbide, copper and titanium. An extra advantage is the speed of the LMD process, compared to other additive manufacturing methods such as those based on a powder bed. The general accuracy of the LMD process amounts to 0.3 mm.

Okuma has introduced LMD technology in two main series of its machining centres, characterised as MU Laser EX and Multus Laser EX. The MU series consists of 5-axis CNC-controlled



The Okuma MU-6300V Laser EX machining centre with additive LMD technology.

machining centres, see Figure 4, the Multus series consists of CNC-controlled turning centres with laser hardening ability.

Combining subtractive and additive manufacturing

The availability of conventional subtractive machining technology with additive technology in one machine means that the workpiece does not need to be transported from one machine to another, thus avoiding reclamping. This results in higher accuracies, shorter throughput times and lower costs.

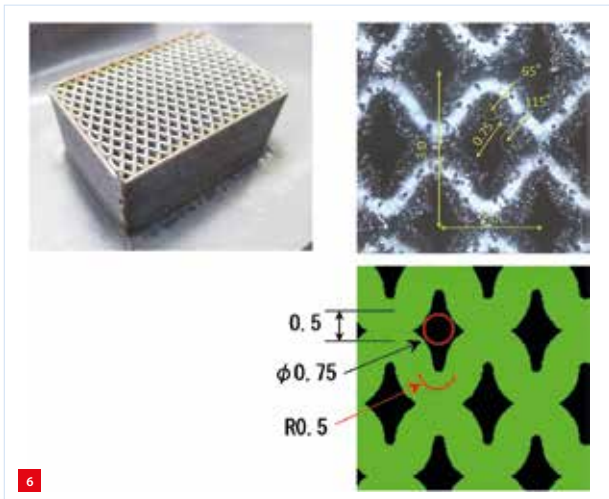
One example of this combination of technologies is the manufacturing and repair of moulds and dies. These include injection moulds, deep-drawing dies and automotive sheet metal tools, see Figure 5. Modifications occur when the shape of a workpiece has to be adapted as a consequence of technical alterations. Generally, the original tool has been produced by means of conventional subtractive methods. However, geometrical modifications can be made by adding material by LMD. Thus, even ribs can be LMD-welded on a tool to improve its stiffness. Where necessary, these ribs can be subtractively finished in a post-process precision action.

The Laser EX machining centres are also able to perform a subtractive action after hardening a workpiece on the spot in the machine, or after modifying a workpiece with LMD technology as described previously. This procedure can be used, for example, for the production of bearing seats on shafts. Here, grinding or turning is applied at the end of the modifying process depending on the required surface quality. In addition, the slots of splines can be milled after LMD or laser-thermal surface treatment.

LMD makes it possible to achieve wall thicknesses of deposited material of as little as 0.5 mm, see Figure 6. In general, the last shaping operation is subtractive, resulting



A both additively and subtractively modified automotive sheet metal tool.



6 An Okuma LMD-produced demonstration grid with 0.5 mm wall thicknesses.

in achieved accuracies equal to the usual precision of subtractive cutting, i.e. grinding and sometimes turning or milling, see Figure 7. Because stacking of many LMD layers might cause an accumulation of vertical inaccuracies, a subtractive action is sometimes integrated between successive LMD additive actions.

To conclude

The foregoing leads to the conclusion that the additive actions of the Laser EX machines provide the same geometric accuracies that are well-known from earlier Okuma machining centres. Consequently, the fruitful combination of the expertise of the Japanese Okuma and the German Trumpf gave the precision engineering world some highly versatile tools: machining centres that manufacture complicated precision products with both subtractive and additive technology. With the extra advantage that heat treatments can be applied right on the spot in the machine.

Source

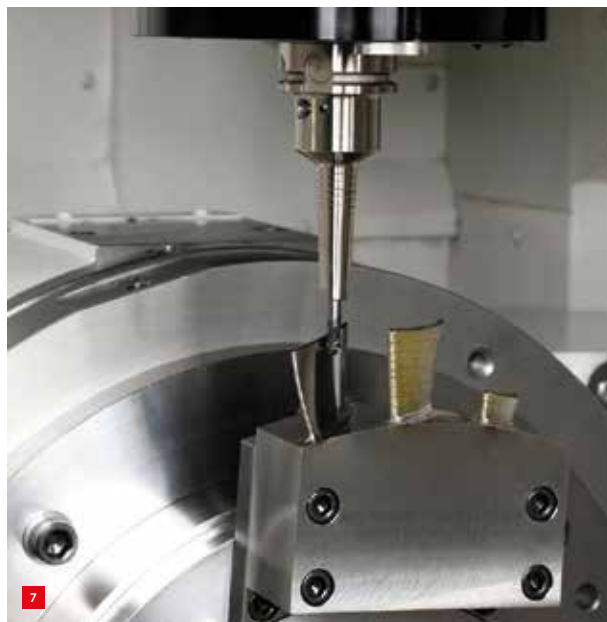
“One tool that does it all”, *Trumpf Laser Community* no. 27, pp. 22-25, November 2018.

INFORMATION

WWW.OKUMA.EU

WWW.GELDERBLOM.NL

WWW.TRUMPF.COM



7 Subtractive finishing of a turbine blade after additive LMD-action.

Dutch Society for Precision Engineering

DSPE

YOUR PRECISION PORTAL

Your button or banner on the website www.DSPE.nl?

The DSPE website is the meeting place for all who work in precision engineering.

The Dutch Society for Precision Engineering (DSPE) is a professional community for precision engineers: from scientists to craftsmen, employed from laboratories to workshops, from multinationals to small companies and universities.

If you are interested in a button or banner on the website www.dspe.nl, or in advertising in Mikroniek, please contact Gerrit Kulsdom at Sales & Services.

DSPE

YOUR PRECISION PORTAL

T: 00 31(0)229-211 211 ■ E: gerrit@salesandservices.nl

ECP² COURSE CALENDAR



COURSE (content partner)	ECP ² points	Provider	Starting date
FOUNDATION			
Mechatronics System Design - part 1 (MA)	5	HTI	30 September 2019
Mechatronics System Design - part 2 (MA)	5	HTI	4 November 2019
Fundamentals of Metrology	4	NPL	to be planned
Design Principles	3	MC	25 September 2019
System Architecting (S&SA)	5	HTI	24 June 2019
Design Principles for Precision Engineering (MA)	5	HTI	25 November 2019
Motion Control Tuning (MA)	6	HTI	27 November 2019
ADVANCED			
Metrology and Calibration of Mechatronic Systems (MA)	3	HTI	29 October 2019
Surface Metrology; Instrumentation and Characterisation	3	HUD	to be planned
Actuation and Power Electronics (MA)	3	HTI	19 November 2019
Thermal Effects in Mechatronic Systems (MA)	3	HTI	3 December 2019
Summer school Opto-Mechatronics (DSPE/MA)	5	HTI	upon request
Dynamics and Modelling (MA)	3	HTI	25 November 2019
Manufacturability	5	LiS	to be planned (Q3/Q4 2019)
Green Belt Design for Six Sigma	4	HI	2 September 2019
RF1 Life Data Analysis and Reliability Testing	3	HI	9 September 2019
Ultra-Precision Manufacturing and Metrology	5	CRANF	16 September 2019
SPECIFIC			
Applied Optics (T2Prof)	6.5	HTI	29 October 2019
Advanced Optics	6.5	MC	19 September 2019
Machine Vision for Mechatronic Systems (MA)	2	HTI	2 July 2019
Electronics for Non-Electronic Engineers – Analog (T2Prof)	6	HTI	to be planned
Electronics for Non-Electronic Engineers – Digital (T2Prof)	4	HTI	to be planned (Q3 2019)
Modern Optics for Optical Designers (T2Prof) - part 1	7.5	HTI	20 September 2019
Modern Optics for Optical Designers (T2Prof) - part 2	7.5	HTI	13 September 2019
Tribology	4	MC	29 October 2019
Basics & Design Principles for Ultra-Clean Vacuum (MA)	4	HTI	11 June 2019
Experimental Techniques in Mechatronics (MA)	3	HTI	25 June 2019
Advanced Motion Control (MA)	5	HTI	18 November 2019
Advanced Feedforward Control (MA)	2	HTI	9 October 2019
Advanced Mechatronic System Design (MA)	6	HTI	to be planned (Q3 2019)
Passive Damping for High Tech Systems (MA)	2.5	HTI	to be planned (Q4 2019)
Finite Element Method	5	ENG	in-company
Design for Manufacturing – Design Decision Method	3	SCHOUT	in-company



ECP² program powered by euspen

The European Certified Precision Engineering Course Program (ECP²) has been developed to meet the demands in the market for continuous professional development and training of post-academic engineers (B.Sc. or M.Sc. with 2-10 years of work experience) within the fields of precision engineering and nanotechnology. They can earn certification points by following selected courses. Once participants have earned a total of 45 points, they will be certified. The ECP² certificate is an industrial standard for professional recognition and acknowledgement of precision engineering-related knowledge and skills, and allows the use of the ECP² title.

WWW.ECP2.EU

Course providers

- Engenia (ENG)
WWW.ENGENIA.NL
- High Tech Institute (HTI)
WWW.HIGHTECHINSTITUTE.NL
- Mikrocentrum (MC)
WWW.MIKROCENTRUM.NL
- LiS Academy (LiS)
WWW.LISACADEMY.NL
- Schout DfM (SCHOUT)
WWW.SCHOUT.EU
- Holland Innovative (HI)
WWW.HOLLANDINNOVATIVE.NL
- Cranfield University (CRANF)
WWW.CRANFIELD.AC.UK
- Univ. of Huddersfield (HUD)
WWW.HUD.AC.UK
- National Physical Lab. (NPL)
WWW.NPL.CO.UK

Content partners

- DSPE
WWW.DSPE.NL
- Mechatronics Academy (MA)
WWW.MECHATRONICS-ACADEMY.NL
- Technical Training for Prof. (T2Prof)
WWW.T2PROF.NL
- Systems & Software Academy (S&SA)

Joining forces in nanomanufacturing

Morphotonics, an indirect spin-off of Philips, is set to join forces with Delft University of Technology's Nano Engineering Research Initiative (NERI) to explore new opportunities of the small scale for breakthrough applications. Morphotonics develops micro- and nanostructure imprint solutions for small and large surfaces. 3D displays, solar panels and LED lighting panels all benefit from nanostructures. Morphotonics imprints these structures on a plate. Due to this nano-imprint manufacturing technology, other high-tech companies will be able to imprint nanostructures at a large scale to enhance various optoelectronic devices.

The collaboration between the parties builds on two mutual interests: advancing precision machines for nano-imprint technology, and the use of nano-imprint technology for the manufacturing and upscaling of micro- and nano-enabled materials and devices. Morphotonics will be active in the NERI themes "Precision Instruments" and "Functional Material Structures".

The ability to manufacture materials and devices in industrially compatible approaches is one of the major challenges in the field of micro- and nanotechnology. NERI has the mission to establish the knowledge and technology foundation "to move nano from lab to app", and to accelerate repeatable and reliable design and manufacturing of relevant functions and applications at an industry-compatible scale. NERI is founded and powered by the multidisciplinary team of scientific experts of TU Delft's Department of Precision and Microsystems Engineering.



The Aurora platform, Morphotonics' state-of-the-art roll-to-plate nano-imprint production line.

WWW.TUDELFT.NL/EN/NER
WWW.MORPHOTONICS.COM



HIGH TECH INSTITUTE



Claus Neeleman (photo), lecturer of this training, has been working as a trainer for some eighteen years. He focuses mainly on practical skills.

SOFT SKILLS & LEADERSHIP

Leadership skills for architects & other technical leaders

You're skilled at developing technology and guiding projects. But knowing the right direction to take is one thing – getting all the stakeholders to buy in is another. And it's a vital skill: if you aren't able to get everyone aligned, you might spend your precious time arguing, eventually even implementing the wrong solutions. You need every stakeholder on board and aligned. This takes influencing and leadership skills.

Our four-day program Leadership skills for architects and other technical leaders will give you the insight and skills you need. Topics are: How to recognise the essential stakeholders you need to get on board? / Design a convincing story / Get every stakeholder on board in the first 3 minutes / Transform resistance into buy-in / Steer for decisions. The training is split into 2 two-day sessions and specifically designed for architects, head engineers, and project leads who want to increase their impact.

Start dates: 6 May 2019 | 25 November 2019

Duration: 2 times 2 days (incl. 2 evening sessions)

Location: Eindhoven

Investment: € 2,565.00 excl. VAT

hightechinstitute.nl/LEADERSHIP



An AM platform for micro-/nanomanufacturing

Nanofabrica, founded in 2016 and based in Tel Aviv, Israel, has recently developed a micron-level resolution additive manufacturing (AM) platform. The company has produced a technological solution that provides an end-to-end solution bespoke to manufacturers requiring micron and sub-micron levels of resolution and surface finish.

According to a Nanofabrica press release, key AM platform developers struggle to get resolution under 50 microns, and the few companies that have strived to provide a micromanufacturing AM solution are either extremely expensive in terms of machine costs and cost per part, or extremely slow, or can only print parts that are very restricted in size.

Killer applications for Nanofabrica's micro-/nano-AM solution can be found in the area of optics, semiconductors, micro-electronics, MEMS, microfluidics, and life sciences. Examples of products include casings for microelectronics, microsprings, micro-actuators and microsensors, and numerous medical applications such as microvalves, microsyringes, and micro-implantable or surgical devices.

Nanofabrica's AM process is based on a technology that is well-known in the AM world, namely a Digital Light Processor (DLP) engine, combined with the use of adaptive optics to achieve repeatable micron levels of resolution. This tool in conjunction with an array of sensors allows for a closed feedback loop. This is the core element that enables Nanofabrica's product to reach very high accuracy while remaining cost-effective as a manufacturing solution. Where all other AM platform developers achieve precision through great hardware, Nanofabrica tackles this issue with

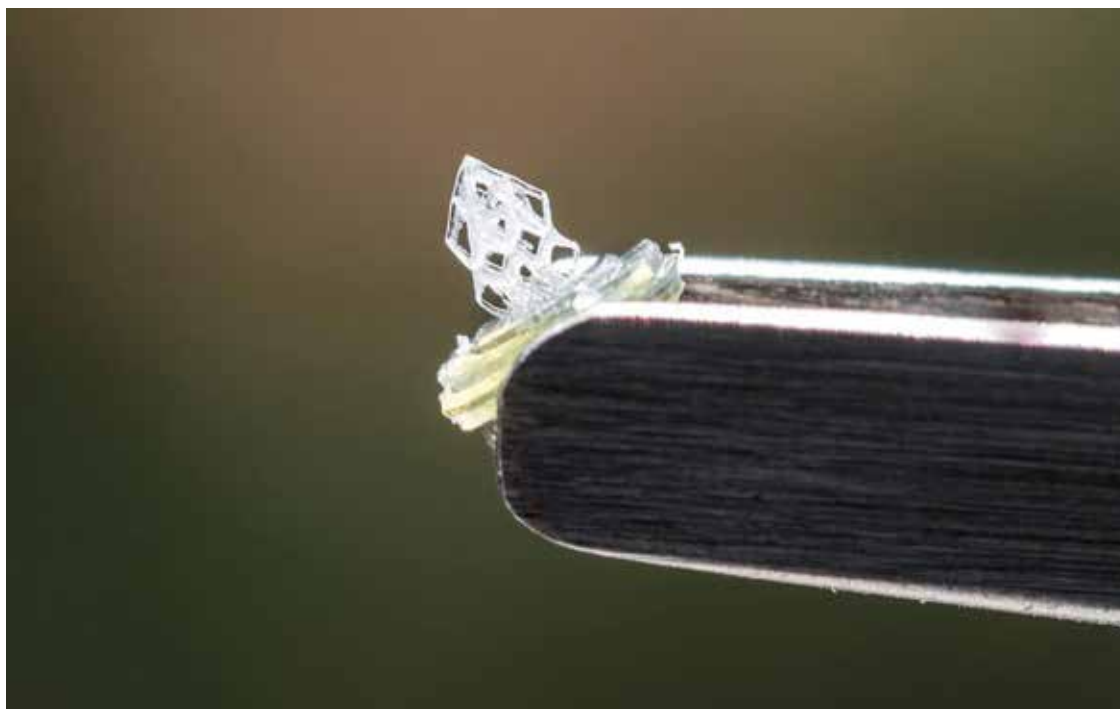
software where solutions are easier, more robust, and less expensive. For adaptive optics, according to Nanofabrica, this is the first time that they have been applied to an AM technology.

To achieve micron resolution over centimetre-sized parts, a number of technologies have been combined. Specifically, the adaptive optics imaging unit has been enhanced with technology and know-how used in the semiconductor industry (where the attainment of micron and sub-micron resolutions over many centimetres is routine.) By working at the intersection of semiconductors and AM, Nanofabrica is able to build large 'macroparts' with intricate microdetails at high speed. To this end, a multi-resolution strategy has been introduced: where fine details are required the parts are printed relatively slowly, but in the areas where the details aren't so exacting, the parts are printed at speeds 10 to 100 times higher. In addition, thousands of small parts can be printed in a single build on the Nanofabrica platform.

The multi-resolution capability is facilitated by the use of hardware which enables a trade-off between speed and resolution, and software algorithms which prepare the part and printing path by defining and sectioning it into low- and high-resolution areas, which are then fed into the printer path and machine parameters. In fact, there is a spectrum of resolutions that allow speed to be optimised while maintaining satisfactory results throughout the part.

Finally, through rigorous R&D, Nanofabrica has managed to develop its own proprietary materials (based on the most commonly used industry polymers) which enable ultra-high resolution.

Nanofabrica advocates close collaboration with customers to optimise outcomes. First and most importantly, the company offers expert design advice to ensure that designs are optimised for its mass-production micromanufacturing AM platform. Interested parties are invited to challenge Nanofabrica with a specific part, work on a proof of concept, and then install the technology either as a commercial manufacturing option, or embedded in an R&D project.



A diamond-shaped lattice in ABS produced by Nanofabrica's AM platform. Part size $0.3 \times 0.3 \times 1 \text{ mm}^3$, print time 45 minutes, and print layer 3 microns. This shape is only possible to manufacture using AM; the structure has ultra-high surface area and is therefore useful in heat dissipators.

WWW.NANO-FABRICA.COM

Larger field of view

Aerotech has introduced the AGV-SPO single pivot-point galvanometer scanner, which enables a larger field of view and reduced spot distortion for critical laser micromachining applications. The new optical design, according to an Aerotech press release, effectively controls the beam entrance pupil to be coincident for the X and Y scanner motion, increasing the effective numerical aperture of the scanner system. This design directly enables a larger field of view for a given focal length and reduces spot distortion over the entire working area. These advantages allow the AGV-SPO to process larger parts faster and with greater consistency.

The AGV-SPO utilises Aerotech's advanced motion and Position Synchronized Output (PSO) capabilities. Contouring functions such as Acceleration Limiting can be used to automatically reduce speeds in tight corners or small radii to minimise overshoot. The laser can be triggered based on the position feedback of the mirrors with PSO to ensure consistent spot overlap as the scanner changes speed.



Aerotech's Infinite Field of View (IFOV) function seamlessly combines servo and scanner motion to extend the marking capability of the scanner across the entire travel range of the servo stages. This eliminates stitching errors that can occur in a more traditional move-expose-repeat process.

WWW.AEROTECH.COM

More AI in MATLAB

Last month, MathWorks, a leading developer of mathematical computing software, introduced Release 2019a with a range of new capabilities in MATLAB and Simulink. MATLAB is a programming environment for algorithm development, data analysis, visualisation, and numeric computation. Simulink is a graphical environment for simulation and model-based design for multi-domain dynamic and embedded systems.

The new release features new products and enhanced capabilities for artificial intelligence (AI), signal processing and static analysis. "One of the key challenges in moving AI from hype to production is that organisations are hiring AI 'experts' and trying to teach them engineering domain expertise", a MathWorks spokesperson explains. "With R2019a, MathWorks enables engineers to quickly and effectively extend their AI skills, whether it's to develop controllers and decision-making systems using reinforcement learning, training deep learning models on NVIDIA DGX and cloud platforms, or applying deep learning to 3-D data."

One of the additions is Reinforcement Learning Toolbox, further enhancing the MATLAB workflow for AI. The new toolbox facilitates a type of machine learning that trains an 'agent' through repeated trial-and-error interactions with an environment to solve controls and decision-making problems.

WWW.MATHWORKS.COM

Cleanroom on campus

Last month, the Brecon Group week delivered a new cleanroom of 1,450 m² to the KMWE Group on the Brainport Industries Campus in Eindhoven (NL). KMWE designs, builds and continuously improves high-tech components, modules and systems based on precision engineering and machining. "The complex project was completed spotlessly, literally and figuratively: completely in accordance with the planning and without any delivery issues. That is thanks to the excellent co-operation between the PP4C Partners: Deerns, Kuijpers PHF Services, WERO Cleanroom Cleaning, CMI and Brecon," says Geerd Jansen, director of the Brecon Group. For ultra-clean workspaces, also known as controlled environments, the PP4C alliance (Professional Partners for Cleanrooms) has been established so that all the disciplines involved work together optimally.

Brecon recently also built a 1,850 m² cleanroom for Anteryon, a manufacturing company that provides innovative optical solutions from idea to mass production for industrial markets. This was the first controlled environment project on the Brainport Industries Campus. Many high-tech companies that establish themselves there need cleanrooms. "The Brecon Group is currently conducting discussions with several newcomers who need a variety of specified cleanrooms", Jansen says.

WWW.KMWE.COM
WWW.ANTERYON.COM
WWW.BRECON.NL
WWW.PP4C.NL



K3D-AddFab scales for industrial additive manufacturing

In 2013, AddLab was one of the first open innovation centres for 3D metal printing in Eindhoven (NL). Last month, partners KMWE, NTS, Machinefabriek De Valk and K3D announced that they were taking their collaboration to the next level, by scaling their shared facility for true series production for applications in high-tech equipment and aerospace. They are also changing the name to K3D-AddFab.

K3D is part of the Kaak Group, an internationally operating manufacturer of bakery equipment, headquartered in Terborg (NL). After the purchase of their first MetalFAB1 from Dutch industrial 3D-printing equipment manufacturer Additive Industries in 2016, K3D have printed more than 45,000 industrial applications. As K3D is the organising partner, K3D-AddFab will be the second centre in their growing distributed manufacturing network in the Netherlands. K3D-AddFab has teamed up

with Additive Industries, which will also provide process & application development support.

The MetalFAB1 system by K3D-AddFab will be installed at the brand-new Brainport Industries Campus (BIC) in Eindhoven. "We are proud to be able to take our unique collaboration in industrial additive manufacturing to the next phase and scale for series production of high-tech equipment parts and aerospace components. The K3D-AddFab team will be an integral part of the K3D network of 3D Printing Centres, allowing for load balancing, volume sharing and materials pooling", said Luuk Wissink, CEO of K3D.

WWW.ADDITIVEINDUSTRIES.COM
WWW.K3D.NL

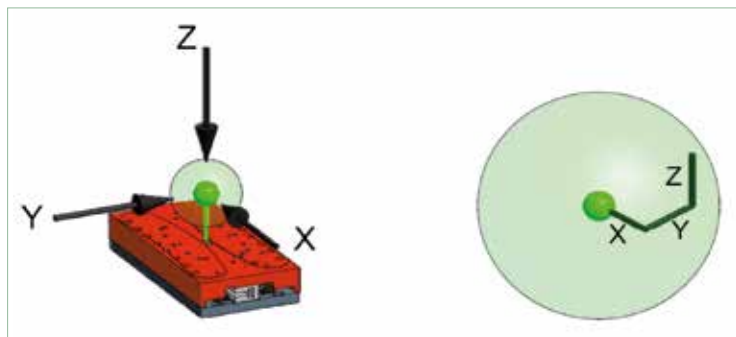
What is the point in precision?

When looking at motion control solutions that provide sub-micron- and nanometer-level accuracy, a new language is necessary, and new standards are required to indicate the real levels of precision that different motion control solutions can achieve. That's the message of ALIO Industries, a leading innovator in (hexapod) motion control technology, based in Arvada, CO, USA.

Recently, ALIO launched the Hybrid Hexapod®, which for the first time provides the ability to achieve repeatable nano-level accuracy, due to its combination of serial and parallel kinematics. To describe precision in this realm, ALIO has introduced the concept of Point Precision®, which has been adopted by NIST (National Institute of Standards and Technology) as the future standard methodology of measuring and quantifying motion systems.



The 6-D ALIO Hybrid Hexapod.



Point Precision metrology: single-point precision.

Point Precision includes all six degrees of freedom of errors of each axis in motion, guaranteeing the precision point in the full work envelope. (As an example, the ALIO patented Hybrid Hexapod has a 3D point precision of less than 100 nm repeatability anywhere in its full work zone.) Point Precision references performance specifications to a point in space, in contrast with the planar methodology current standards use.

While there are compensation methods to reduce error sources in conventional 6-link hexapods, they do not improve performance at the single-digit micron or nanometer level, so ALIO claims. Motion systems' straightness and repeatability performance must be analysed and specified using a 'point precision' methodology that accounts for all 6-D spatial errors in order to provide a true representation of nanometer precision.

WWW.ALIOINDUSTRIES.COM

Start of Software Competence Centre

Last month marked the opening of the Software Competence Centre at the Brainport Industries Campus in Eindhoven (NL). At the official opening ceremony, the centre was awarded the Smart Industry fieldlab status. Fieldlabs are practical environments in which companies and knowledge institutions purposefully develop, test and implement Smart Industry (Industrie 4.0) solutions. They also form an environment in which people learn to apply these solutions. In addition, they strengthen links with research, education and government. The new high-tech software fieldlab will work on innovating in software and using software to drive innovation in industry, including in areas such as digital twinning and model-based engineering.

The fieldlab is an initiative by a consortium of high-tech software companies in the areas of virtual prototyping & design, model-based software, and data analytics & services. Paul van Nunen, CEO of Brainport Development, emphasised the power of the Brainport region working together on the latest developments. "What could be better than software playing such a central role in the middle of the factory of the future, i.e. this campus? Companies from Brainport understand that they have to go along with the trend for the further merging of hardware and software. And vocational students, who are following technical training here, learn that tinkering is just as much about nuts and bolts as it is about encryption or machine learning, for example."

WWW.HIGHTECHSOFTWARECLUSTER.NL

Inspection of precision etching

Leading photochemical etching specialists, Precision Micro, headquartered in Birmingham, UK, has installed a further automated optical inspection machine (AOI) as part of its on-going and extensive investment program to meet the upturn in demand for high-volume, close-tolerance precision-etched components. Precision Micro has a 50-year pedigree in photo etching, a highly precise, tightly controlled corrosion process used to produce complex, burr- and stress-free metal components with very fine detail.

The new system has been specified to enhance verified part quality and automation for discrete components and can handle material thicknesses down to 0.2 mm (200 microns). Unlike its current systems, Precision Micro's new AOI is able to undertake complete 100% visual and dimensional inspection on both sides of the product, auto-bagging defect-free components ready for dispatch.

The machine uses high-definition cameras and a variety of lighting sources to scan and photograph components, comparing the captured image with the pre-programmed CAD data. This ensures any differences between original design intent and the actual nature of the manufactured part are immediately detected. Up to 1,000,000 components can be inspected in just 48 hours.

WWW.PRECISIONMICRO.COM

POSITIONING SYSTEMS REIMAGINED... INTEGRATED GRANITE MOTION SYSTEMS FROM AEROTECH

IGM Systems as an Alternative to Conventional Stage-on-Granite

Advantages Include:

- Air-bearing and mechanical-bearing axes
- Ball-screw drives or linear motors
- High stiffness as well as reduced height for increased design flexibility
- Customisation of travel, payload, and dynamic performance



Visit us at the international trade fair for quality assurance from 7 -10 May 2019 in Stuttgart. You will find us in hall 5, booth 5218.



Visit aerotech.co.uk or Call +44 1256 855055

AH0119B-PMG-LTD

PRECISION-IN-BUSINESS DAY PREVIEW: NTS

Over the past 25 years, NTS has developed into a first-tier systems supplier in optomechatronic systems and mechanical modules for large, high-tech machine manufacturers (OEMs). The opening of the new NTS Campus in Eindhoven (NL) is another step in NTS's effort to further integrate the competences of Development & Engineering (D&E), Component Manufacturing and System Assembly in order to accelerate the time-to-market for its customers.

To acknowledge these developments, NTS will be hosting a DSPE Precision-in-Business Day (in fact an afternoon) on Thursday, 23 May 2019, on the NTS Campus.

Programme

- Introduction NTS
Rob Karsmakers, COO NTS
- Adding customer value by combining Development & Engineering competences and industrial operations
Hans Scholtz, managing director Development & Engineering division at NTS
- System architect as intermediate between two roadmaps
Rens van den Braber, system architect at NTS

- DfX as the link between Development & Engineering and NPI
Ivan van der Kroon, system engineer at NTS
- NTS Campus tour



Artist's impression of NTS Precision's new housing on the NTS Campus.

WWW.NTS-GROUP.NL

WWW.DSPE.NL/EVENTS/PIB-EVENTS (REGISTRATION)

SAVE THE DATE: 27 JUNE 2019

ENGINEERING FOR PARTICLE CONTAMINATION CONTROL

Contamination control has become a highly relevant knowledge area in precision engineering. Therefore, DSPE is organising a specific Knowledge Day on Engineering for Particle Contamination Control on 27 June 2019. The primary focus will be on design



Particle contamination control is an issue during the design, assembly and operation of advanced machinery. Photo: VDL ETG

aspects aimed at dealing with particle contamination or minimising the implications of particle contamination. In addition, information will be shared regarding simulation tools and other tooling that support the design (and test) phase of a project, as well as practical measures for particle contamination control during the production and assembly of precision systems.

The DSPE Knowledge Day on Engineering for Particle Contamination Control is organised in collaboration with VCCN (Association of Contamination Control Netherlands) and DSPE members VDL ETG, NTS, Thermo Fisher Scientific and Brecon Group. Doors open on 27 June from 13:00, with the session starting at 13:30. The event is being held at Fontys University of Applied Sciences in Eindhoven (NL).

WWW.DSPE.NL/EVENTS/AGENDA (INFORMATION & REGISTRATION)

Air Bearings



AeroLas GmbH
Grimmerweg 6
D-82008 Unterhaching
Germany

T +49 89 666 089-0
F +49 89 666 089-55
E info@aerolas.de
W www.aerolas.de

AeroLas is world leader in air bearing technology strengthening the customer's competitive advantage with customized air-guided products and solutions.

Automation Technology



Festo BV
Schieweg 62
2627 AN DELFT
The Netherlands
T +31 (0)15-2518890
E sales@festo.nl
W www.festo.nl
Contact person:
Mr. Ing. Richard Huisman

Festo is a leading world-wide supplier of automation technology and the performance leader in industrial training and education programs.

member **DSPE**

Cleanrooms

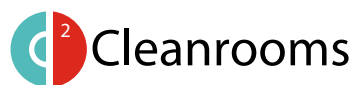


Brecon Group
Droogdokkeniland 7
5026 SP Tilburg
T +31 (0)76 504 70 80
E brecon@brecon.nl
W www.brecon.nl

Brecon Group can attribute a large proportion of its fame as an international cleanroom builder to continuity in the delivery of quality products within the semiconductor industry, with ASML as the most important associate in the past decades.

Brecon is active with cleanrooms in a high number of sectors on:
* Industrial and pharmaceutical
* Healthcare and medical devices

member **DSPE**



Connect 2 Cleanrooms BV
Newtonlaan 115
Zen Building
3584 BH Utrecht
Nederland
T +31 (0)30 210 60 51
E info@connect2cleanrooms.com
W www.connect2cleanrooms.nl

Our cleanroom solutions are bespoke and scalable, encouraging efficiency through flexible design. We help organisations reduce failure rates by getting it right first time.

member **DSPE**

Development



TNO
T + 31 (0)88-866 50 00
W www.tno.nl

TNO is an independent innovation organisation that connects people and knowledge in order to create the innovations that sustainably boosts the competitiveness of industry and wellbeing of society.

member **DSPE**

Development and Engineering



Segula Technologies Nederland B.V.
De Witbogt 2
5652 AG Eindhoven
T +31 (0)40 8517 500
W www.segula.nl

SEGULA Technologies Nederland BV develops advanced intelligent systems for the High Tech and Automotive industry. As a project organisation, we apply our (engineering) knowledge to non-linear systems. This knowledge is comprised of systems architecture and modelling, analysis, mechanics, mechatronics, electronics, software, system integration, calibration and validation.

member **DSPE**

Education



Leiden school for Instrumentmakers (LiS)
Einsteinweg 61
2333 CC Leiden
The Netherlands
T +31 (0)71-5681168
E info@lis.nl
W www.lis.nl

The LiS is a modern level 4 MBO school with a long history of training Research instrumentmakers. The school establishes projects in cooperation with industry and scientific institutes thus allowing for professional work experience for our students. LiS TOP accepts contract work and organizes courses and summer school programs for those interested in precision engineering.

member **DSPE**

YOUR COMPANY PROFILE IN THIS GUIDE?

Please contact:
Sales & Services
Gerrit Kulsdom / +31 (0)229 211 211
gerrit@salesandservices.nl

Electrical Discharge Machining (EDM)



CVT BV

Heiberg 29C
5504 PA Veldhoven
The Netherlands
T +31 (0)497 54 10 40
E info@cvtbv.nl
W www.heinmade.com

Partner high tech industry for wire EDM precision parts. Flexible during day shifts for prototyping. Outside office hours low cost unmanned machining. Call and enjoy our expertise!

member **DSPE**



Ter Hoek Vonkerosie

Propaanstraat 1
7463 PN Rijssen
T +31 (0)548 540807
F +31 (0)548 540939
E info@terhoek.com
W www.terhoek.com

INNOVATION OF TOMORROW,
INSPIRATION FOR TODAY
Staying ahead by always going the extra mile. Based on that philosophy, Ter Hoek produces precision components for the high-tech manufacturing industry.

We support customers in developing high-quality, custom solutions that can then be series-produced with unparalleled accuracy. That is what makes us one of a kind.

It is in that combination of innovative customization and repeated precision that we find our passion. Inspired by tomorrow's innovation, each and every day.

member **DSPE**

Lasers, Light and Nanomotion



Laser 2000 Benelux C.V.

Voorbancken 13a
3645 GV Vinkeveen
Postbus 20, 3645 ZJ Vinkeveen
T +31(0)297 266 191
F +31(0)297 266 134
E info@laser2000.nl
W www.laser2000.nl

Laser 2000 Benelux considers it her mission to offer customers the latest photonics technologies available. Our areas of expertise are:

- Lasers, scanners and laser machines for industry and research
- Light metrology instruments for LED and luminaire industries
- Light sources for scientific applications
- Piezo- and stepper motion products for nano- and micro positioning
- Inspection and research grade high speed cameras
- Laser safety certified products



Te Lintelo Systems B.V.

Mercurion 28A
6903 PZ Zevenaar
T +31 (0)316 340804
E contact@tlsbv.nl
W www.tlsbv.nl

Photonics is our passion! Our experienced team is fully equipped to assist you with finding your best optical business solution. For over 35 years TLS represent prominent suppliers in the photonics industry with well-educated engineers, experience and knowledge. Over the years we became the specialist in the field of:

- Lasers
- Light metrology,
- Opto-electronic equipment,
- Positioning equipment
- Laser beam characterization and positioning,
- Interferometry,
- (Special) Optical components,
- Fiber optics,
- Laser safety

Together with our high end suppliers we have the answer for you!

Mechatronics Development



SOURCE OF YOUR TECHNOLOGY

Sioux CCM

De Pinckart 24
5674 CC Nuenen
T +31 (0)40 2635000
F info.ccm@sioux.eu
W www.siox.eu

Sioux CCM is a technology partner with a strong focus on mechatronics.

We help leading companies with the high-tech development, industrialization and creation of their products, from concept stage to a prototype and/or delivery of series production. Commitment, motivation, education and skills of our employees are the solid basis for our business approach

Sioux CCM is part of the Sioux Group.

member **DSPE**



Manufacturing Technical Assemblies (MTA) b.v.

Waterbeemd 8
5705 DN Helmond
T +31 (0)492 474992
E info@m-t-a.nl
W www.m-t-a.nl

MTA is an high-tech system supplier specialized in the development and manufacturing of mechatronic machines and systems.

Our clients are OEM s in the Packaging, Food, Graphics and High-tech industries.

member **DSPE**

Mechatronics Development



MI-Partners
Dillenburgstraat 9N
5652 AM Eindhoven
The Netherlands
T +31 (0)40 291 49 20
F +31 (0)40 291 49 21
E info@mi-partners.nl
W www.mi-partners.nl

MI-Partners is active in R&D of high-end mechatronic products and systems. We are specialised in concept generation and validation for ultra-fast (>10g), extremely accurate (sub-nanometers) or complex positioning systems and breakthrough production equipment.

member **DSPE**

Metal Precision Parts



Etchform BV
Arendstraat 51
1223 RE Hilversum
T +31 (0)35 685 51 94
F info@etchform.com
W www.etchform.com

Etchform is a production and service company for etched and electroformed metal precision parts.

member **DSPE**

Micro Drive Systems

maxon motor
driven by precision

maxon motor benelux
Josink Kolkweg 38
7545 PR Enschede
The Netherlands
F +31 53 744 0 713
E info@maxonmotor.nl
W www.maxonmotor.nl

maxon motor is a developer and manufacturer of brushed and brushless DC motors as well as gearheads, encoders, controllers, and entire precision drive systems. maxon motor is a knowledge partner in development. maxon drives are used wherever the requirements are particularly high: in NASA's Mars rovers, in surgical power tools, in humanoid robots, and in precision industrial applications, for example. Worldwide, maxon has more than 2,500 employees divided over sales companies in more than 40 countries and eight production locations: Switzerland, Germany, Hungary, South Korea, France, United States, China and The Netherlands.

member **DSPE**

Micro Drive Systems



FAULHABER Benelux B.V.
Drive Systems
High Tech Campus 9
5656 AE Eindhoven
The Netherlands
T +31 (0)40 85155-40
E info@faulhaber.be
E info@faulhaber.nl
W www.faulhaber.com

FAULHABER specializes in the development, production and deployment of high-precision small and miniaturized drive systems, servo components and drive electronics with output power of up to 200 watts. The product range includes brushless motors, DC micromotors, encoders and motion controllers. FAULHABER also provides customer-specific complete solutions for medical technology, automatic placement machines, precision optics, telecommunications, aerospace and robotics, among other things.



Physik Instrumente (PI) Benelux BV
Hertog Hendrikstraat 7a
5492 BA Sint-Oedenrode
The Netherlands
T +31 (0)499-375375
F +31 (0)499 375373
E benelux@pi.ws
W www.pi.ws

Stay ahead with drive components, positioners and systems by PI. In-depth knowledge, extensive experience and the broadest and deepest portfolio in high-end nanopositioning components and systems provide leading companies with infinite possibilities in motion control.

member **DSPE**

Motion Control Systems



Aerotech United Kingdom
The Old Brick Kiln
Ramsdell, Tadley
Hampshire RG26 5PR
UK
T +44 (0)1256 855055
F +44 (0)1256 855649
W www.aerotech.co.uk

Aerotech's motion control solutions cater a wide range of applications, including medical technology and life science applications, semiconductor and flat panel display production, photonics, automotive, data storage, laser processing, electronics manufacturing and testing.



Newport Spectra-Physics B.V.
Vechtensteinlaan 12 - 16
3555 XS Utrecht
T +31 (0)30 6592111
E netherlands@newport.com
W www.newport.com

Newport Spectra-Physics B.V. is a subsidiary of Newport, a leader in nano and micro positioning technologies with an extensive catalog of positioning and motion control products. Newport is part of MKS Instruments Inc., a global provider of instruments, subsystems and process control solutions that measure, control, power, monitor, and analyze critical parameters of advanced processes in manufacturing and research applications.

member **DSPE**

Motion Control Systems



Physik Instrumente (PI) Benelux BV

Hertog Hendrikstraat 7a
5492 BA Sint-Oedenrode
The Netherlands
T +31 (0)499-375375
F +31 (0)499 375373
E benelux@pi.ws
W www.pi.ws

Opt for state-of-the-art motion control systems from the world's leading provider PI. Developed, manufactured and qualified in-house by a dedicated and experienced team. Our portfolio includes a wide and deep range of components, drives, actuators and systems and offers infinite possibilities in motion control on a sub-micron and nanometer scale.

member **DSPE**

Optical Components



Molenaar Optics

Gerolaan 63A
3707 SH Zeist
T +31 (0)30 6951038
E info@molenaar-optics.nl
W www.molenaar-optics.eu

Molenaar Optics is offering optical engineering solutions and advanced products from world leading companies OptoSigma, Sill Optics and Pyser Optics.

member **DSPE**

Precision Electro Chemical Machining



Ter Hoek Applicatie Centrum B.V.

Propaanstraat 1
7463 PN Rijssen
T +31 (0)548 540807
F +31 (0)548 540939
E info@terhoek.com
W www.terhoek.com

As Application Centre we possess the required knowledge to support our clients in every phase of development and process selection. With our own PEM800 machine we can also use PECM in-house for the benefit of our clients.

member **DSPE**

Piezo Systems



HEINMADE BV

Heiberg 29C
NL - 5504 PA Veldhoven
T +31 (0)40 851 2180
E info@heinmade.com
W www.heinmade.com

As partner for piezo system solutions, HEINMADE serves market leaders in the high tech industry. Modules and systems are developed, produced and qualified in-house. HEINMADE distributes Noliac piezo components.

member **DSPE**

Piezo Systems



Physik Instrumente (PI) Benelux BV

Hertog Hendrikstraat 7a
5492 BA Sint-Oedenrode
The Netherlands
T +31 (0)499-375375
F +31 (0)499 375373
E benelux@pi.ws
W www.pi.ws

High-precision piezo systems and applications that perform on a sub-micron and nanometer scale: world leader PI develops, manufactures and qualifies these in-house. With a broad and deep portfolio with infinite possibilities in components, drives, actuators and systems at hand, our experienced team is dedicated to find the best solution for any motion control challenge.

member **DSPE**

Ultra-Precision Metrology & Engineering



IBS Precision Engineering

Esp 201
5633 AD Eindhoven
T +31 (0)40 2901270
F +31 (0)40 2901279
E info@ibspe.com
W www.ibspe.com

IBS Precision Engineering delivers world class measurement, positioning and motion systems where ultra-high precision is required. As a strategic engineering partner to the world's best manufacturing equipment and scientific instrument suppliers, IBS has a distinguished track record of proven and robust precision solutions. Leading edge metrology is at the core of all that IBS does. From complex carbon-fibre jet engine components to semiconductor chips accurate to tens of atoms; IBS has provided and engineered key enabling technologies.

member **DSPE**

ADVERTISERS INDEX

■ Aerotech	45	■ Mikroniek Guide	47 - 50
www.aerotech.co.uk			
■ Faulhaber	10	■ NTS-Group	11
www.faulhaber.com/p/bxt/en		www.nts-group.nl	
■ Heidenhain Nederland BV	Cover 4	■ Oude Reimer BV	25
www.heidenhain.nl		www.oudereimer.nl	
■ High Tech Institute	41	■ Segula	31
www.hightechinstitute.nl/leadership		www.segula.nl	
■ IBS Precision Engineering BV	11	■ Ter Hoek Application Centre	18
www.ibspe.com		www.terhoek.com	
■ Maxon motor	36	■ Tempcontrol	Cover 2
www.maxonmotor.nl		www.tempcontrol.nl	

DSPE
YOUR PRECISION PORTAL



MIKRONIEK
PROFESSIONAL JOURNAL ON PRECISION ENGINEERING

Mikroniek is the professional journal on precision engineering and the official organ of the DSPE, The Dutch Society for Precision Engineering.

Mikroniek provides current information about technical developments in the fields of mechanics, optics and electronics and appears six times a year.

Subscribers are designers, engineers, scientists, researchers, entrepreneurs and managers in the area of precision engineering, precision mechanics, mechatronics and high tech industry. Mikroniek is the only professional journal in Europe that specifically focuses on technicians of all levels who are working in the field of precision technology.

Publication dates 2019

nr.:	deadline:	publication:	theme (with reservation):
3.	17-05-2019	21-06-2019	Design principles
4.	02-08-2019	06-09-2019	Manufacturability
5.	20-09-2019	25-10-2019	Precision sensors (incl. preview Precision Fair 2019)
6.	08-11-2019	13-12-2019	Energy technology (micro & macro)

For questions about advertising, please contact Gerrit Kulsdom
T: 00 31(0)229-211 211 ■ E: gerrit@salesandservices.nl ■ I: www.salesandservices.nl



HEIDENHAIN



Exposed Linear Encoders for Permanently Stable Measured Values

Machines in electronics manufacturing, in high-level automation, or medical technology need to position finely, quickly and exactly. Exposed linear encoders from HEIDENHAIN are used exactly wherever there is a need for positioning with extremely high accuracy or for precisely defined movements. Even if the encoder is subjected to contamination, the scanning signals stay lastingly stable. This is ensured by the new HEIDENHAIN signal processing ASIC, which almost completely compensates signal changes caused by contamination and maintains the encoder's original signal quality. And this without any significant increase in the noise component or interpolation error of the scanning signals, so the control loop receives highly accurate absolute or incremental position information permanently and reliably.

HEIDENHAIN NEDERLAND B.V.

6716 BM Ede, Netherlands

Telephone 0318-581800

www.heidenhain.nl

Angle Encoders + Linear Encoders + Contouring Controls + Position Displays + Length Gauges + Rotary Encoders